BOREAS An international journal of Quaternary research

Chironomid-inferred summer temperature development during the late Rissian glacial, Eemian interglacial and earliest Würmian glacial at Füramoos, southern Germany

ALEXANDER BOLLAND, OLIVER A. KERN, ANDREAS KOUTSODENDRIS, JÖRG PROSS AND OLIVER HEIRI

BOREAS

Bolland, A., Kern, O. A., Koutsodendris, A., Pross, J. & Heiri, O.: Chironomid-inferred summer temperature development during the late Rissian glacial, Eemian interglacial and earliest Würmian glacial at Füramoos, southern Germany. *Boreas*. https://doi.org/10.1111/bor.12567. ISSN 0300-9483.

Eemian pollen records from central Europe describe a transition from thermophilous tree taxa in the early Eemian to boreal tree taxa in the late Eemian with forest opening in the subsequent stadial. Available summer-temperature reconstructions for the mid- to late Eemian transition show decreasing values during that time. We present a new chironomid record from southern Germany that covers the mid-Eemian to the end of the first Würmian stadial (*c*. 125–105 ka) and also parts of the late Rissian glaciation and early Brörup interstadial of the early Würmian glaciation. Based on this record we describe lake development in the former Füramoos palaeolake and quantitatively reconstruct July air temperature during the examined interval. Late Rissian sediments are dominated by two chironomid taxa, *Sergentia coracina-type* and *Micropsectra radialis-type,* indicating very cold conditions. Following an uncertain interval, probably including a hiatus at the late Rissian/Eemian transition, mid-Eemian sediments contain *Tanytarsus glabrescens-type* and *Tanytarsus mendax-type* suggesting relatively high July air temperatures. During the late Eemian, typically thermophilic taxa such as *Tanytarsus glabrescens-type* disappear, suggesting decreasing temperatures. Stadial A is associated with increases in *Microtendipes pedellus-type* suggesting more oligotrophic conditions. Early Brörup sediments contain *Tanytarsus glabrescens-type,* suggesting a slight increase in July air temperature. Reconstructed July air temperatures show temperatures of 7–8 °C during the late Rissian and a decline from ~15.5–12 °C during the mid- to late Eemian associated with decreasing Northern Hemisphere July insolation. July air temperature values vary between 12 and 14 °C in the late Eemian, while reconstructed temperatures remain within 12–13.5 °C during Stadial A. Our new chironomid-based temperature reconstruction provides valuable corroboration and new quantification of temperature development from the mid-Eemian to the early Brörup interstadial as well as for sections of the late Rissian from the alpine foreland of southern Germany.

Alexander Bolland (alexanderwilliam.bolland@unibas.ch) and Oliver Heiri, Geoecology, Department of Environmental Sciences, University of Basel, Klingelbergstrasse 27, CH-4056 Basel, Switzerland; Oliver A. Kern, Andreas Koutsodendris and Jörg Pross, Paleoenvironmental Dynamics Group, Institute of Earth Sciences, Heidelberg University, Im Neuenheimer Feld 234, D-69120 Heidelberg, Germany; *received 21st March 2021, accepted 5th October 2021.*

During the last interglacial interval, the Eemian, global temperatures were 1–2 °C higher than pre-industrial values (Turney & Jones 2010; Masson-Delmotte *et al*. 2013; Otto-Bliesner *et al*. 2013) and as a result of large-scale deglaciation sea level was 6–9 m higher than today (Dutton *et al*. 2015). The Eemian is broadly correlated to Marine Isotope Stage (MIS) 5e (Dansgaard *et al*. 1993) but there is a *c*. 6000-year lag between the onset of MIS 5e and afforestation in some terrestrial records from central Europe (Shackleton *et al*. 2003). Transition from the penultimate (i.e. Rissian) glacial to the Eemian was characterized by greenhouse gas concentrations rising on a global scale (Lüthi *et al*. 2008; Schilt *et al*. 2010) and increasing Northern Hemisphere summer insolation (Berger & Loutre 1991).

Terrestrial records from central Europe identify the Eemian as a heavily forested interval chronologically between the open landscapes of the previous Rissian glacial and the first phase of forest opening in the following glacial complex (Turner & West 1968). Over large parts of Europe, steppic tundras associated with the penultimate, Rissian glaciation transitioned into forest biomes at the onset of the Eemian (e.g. Litt 1994). Eemian vegetation reconstructions for central Europe indicate a characteristic succession of arboreal taxa, broadly described in three phases by Klotz *et al*. (2003) as the early Eemian *Pinus–Quercetum mixtum–Corylus* phase, the mid-Eemian *Carpinus–Picea* phase and finally the late-Eemian *Pinus–Picea–Abies* phase, although regional disparities exist between the available pollen records. The end of the Eemian in central Europe is characterized by a strong increase in the percentages of herbs, and particularly Poaceae, at the expense of tree-pollen percentages that marks the onset of the last glacial period (e.g. Woillard 1978; Müller *et al*. 2003).

For terrestrial environments in Europe, quantitative proxy-based temperature reconstructions for the Eemian interglacial and Würmian glacial periods have been produced from pollen (e.g. Kühl & Litt 2003; Kühl *et al*. 2007), beetle (Ponel 1995; Walkling & Coope 1996; Behre *et al*. 2005) and chironomid assemblages (Engels *et al*. 2008, 2010, 2014; Plikk *et al*. 2019; Bolland *et al*. 2020; Ilyashuk *et al*. 2020). The use of multiple proxies for temperature estimation is vital for understanding continental temperature development because different proxies can respond differently to environmental forcing factors

DOI 10.1111/bor.12567

(Lotter *et al.* 2012). Hence, by utilizing multiple proxies it is possible to develop an integrated picture of past climatic change, ideally identifying and separating the influence of different seasonal variables such as summer temperature, winter temperature and continentality.

The fossil remains of chironomid larvae are an excellent proxy for reconstructing environmental change, being ubiquitous, diverse, nearly eurytopic as a family and remaining well preserved in lacustrine sediments (Brooks *et al.* 2007). They allow the assessment of in-lake environmental change through time and, because of the close relationships of many chironomid taxa with summer air temperatures, can be used to quantitatively reconstruct mean July air temperature by numerically relating the fossil assemblages to modern assemblage and temperature data (Brooks 2006; Eggermont & Heiri 2012). Here we present a new chironomid record covering sections of the late Rissian, Eemian and early Würmian from Füramoos, southern Germany, to infer environmental change in the Füramoos palaeolake and produce a chironomid-based July air temperature reconstruction. Our new record yields a stratigraphically well constrained, centennial-scale temperature reconstruction from the mid-Eemian (*c.* 125 ka) to the end of Stadial A (*c.* 104.5 ka), thus covering the transition from the mid-Eemian to the late Eemian and the subsequent Stadial A. Our record also provides insights into July air temperatures during the Late Rissian glaciation, prior to the onset of the Eemian and the early Brörup interstadial that follows Stadial A, although these sections of our record are less well constrained by the available chronological data.

The study site

The Füramoos Ried peat bog (Fig. 1) was formed in a basin between two Rissian glacial moraines in the German alpine foreland (Schreiner 1996; Busschers *et al.* 2008) situated at 662 m a.s.l. Its sediments represent a nearly continuous archive of environmental change from the end of the Rissian glaciation to the Holocene (Schreiner 1982; Müller *et al.* 2003; Winterholler 2004; Kern *et al.* 2019). The modern mean July air temperature of the German alpine foreland region is between 16–18 °C for the period 1961–1990 (https://www.dwd.de) and mean July air temperatures of 17.8 °C have been recorded at Memmingen, 20 km from Füramoos between 610–615 m a.s.l. for the period 1991–2020 (DWD Climate Data Centre 2021). The study is based on the sediment core Fu15-2, retrieved from Füramoos at latitude 47°59′26.149″N, longitude 9°53′13.318″E in 2015 using a mobile drilling rig.

In this study we describe the results from a single sediment core segment Fu15-2 790–890 cm (hereafter referred to as 'Fu15-2 core') that contains sediments from the Rissian glaciation, Eemian interglacial, Stadial A and early Brörup interstadial (Fig. 2). The sediment core has previously been correlated to the record of Müller *et al.* (2003), also from Füramoos (Becker 2018; Kern *et al.* 2019). These correlations indicate that the sediment between 890 and 856 cm is from the Rissian glacial and consists primarily of grey clays with some fine sand grains. There then appears to be a hiatus in the sediment core at 856 cm (see Discussion) seen in the lithology as an abrupt change from Rissian glacial clays to Eemian fen peat. Sediments from 855 to 837 cm are diagnosed as fen peats because they are highly organic and contain a high proportion of inorganic clastic material (Kern *et al.* 2019), while the microfossil content clearly indicates that sedimentation took place under water in lacustrine conditions (Fig. 3). The fen peat is believed to have formed due to the increased deposition rates of detritus originating from aquatic macrophytes and near-shore terrestrial vegetation relative to algal organic matter or other aquatic sediment components during these intervals, possibly related to changing productivity in the littoral or open water of the lake, or changes in the relevant transport processes for these sediment components to the coring site. At 837 cm there is a transition to highly organic lacustrine muds until 819 cm. Sediments within the section 856–819 cm are largely homogenous, and due to the high degree of humification individual plant remains cannot be identified (Kern *et al.* 2019). Sediments from depths 819–803 cm are low-organic lacustrine muds that correspond to Stadial A and sediments from depths 803–790 cm are fen peat corresponding to the Brörup interglacial, again, based on the microfossil content, clearly deposited under water in lacustrine conditions. Macroscopically, sediment layers from the Brörup form plates of organic-rich, highly humified sediments that can be easily separated from one another in layers but remain difficult to bend or break individually.

Material and methods

Pollen sample preparation and analysis

For the present study, eight pollen samples were processed across the transition from Rissian glacial sediments to Eemian fen peat (857–851 cm; 1-cm resolution; Fig. 2). These samples complement the previously available, low-resolution (12 cm) palynological data set for the same core segment examined by Becker (2018; Fig. 2), making 20 pollen samples in total. This was done to examine an uncertain sediment interval, 857–851 cm, and confirm the hiatus at 856 cm as the original low resolution vegetation reconstruction (Becker 2018) did not capture the first vegetation stages of the Eemian interglacial interval at Füramoos. Specifically these additional analyses confirmed that intervals of *Betula* and *Pinus* dominance and *Quercus* dominance, displayed in Müller *et al.* (2003) were absent from the Fu15-2 core (see below).

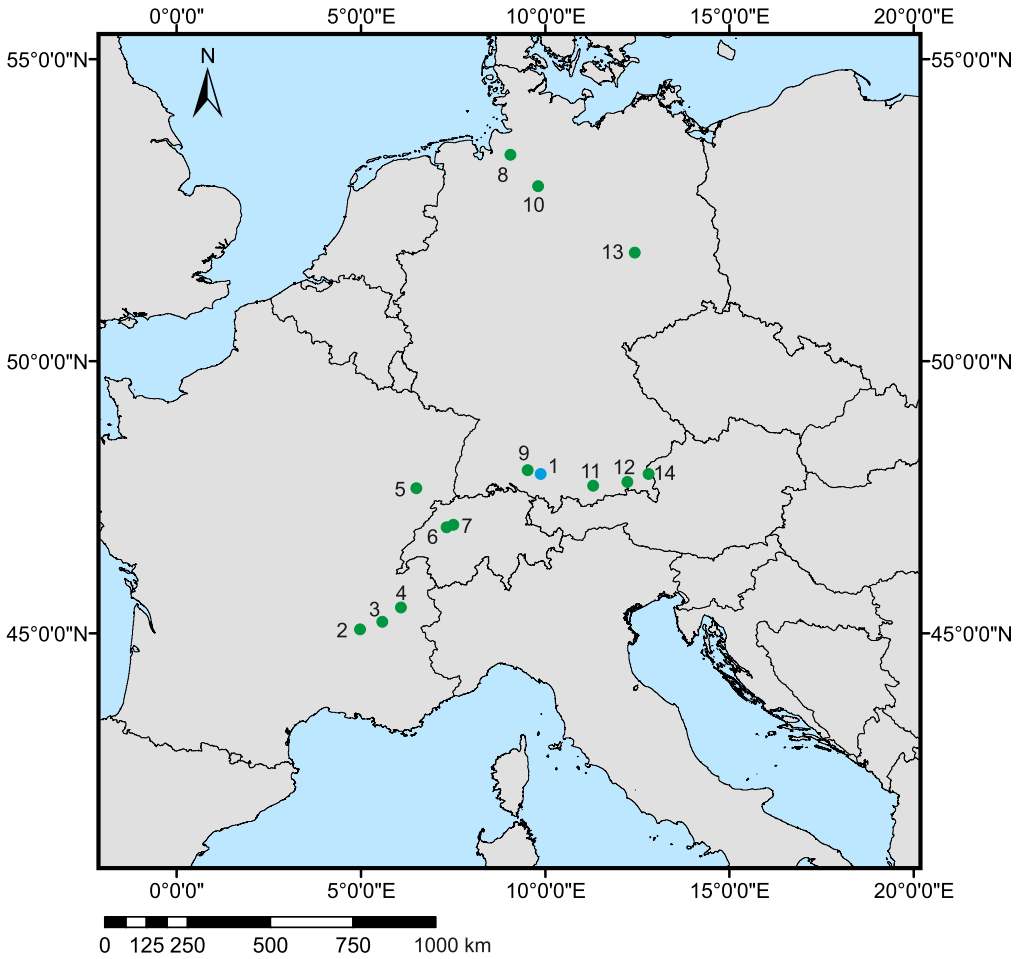

Fig. 1. Site locations of temperature reconstructions in central Europe referred to in the text for the interval from the Rissian glacial interval to the Brörup interstadial: 1 = Füramoos (blue circle; Klotz *et al.* 2003, 2004; Müller *et al.* 2003; this study); 2 = Les Echets (Klotz *et al.* 2004); 3 = La Flachère (Klotz *et al.* 2003); 4 = Lathuile (Klotz *et al.* 2003); 5 = La Grande Pile (Woillard 1978; Ponel 1995; Kühl & Litt 2003; Klotz *et al.* 2004); 6 = Meikirch II (Klotz *et al.* 2003); 7 = Beerenmösli (Klotz *et al.* 2003); 8 = Oerel (Behre *et al.* 2005); 9 = Jammertal (Müller 2000; Klotz *et al.* 2003, 2004; Müller *et al.* 2005); 10 = Bispingen (Kühl & Litt 2003); 11 = Eurach (Klotz *et al.* 2003); 12 = Samerberg (Grüger 1979; Klotz *et al.* 2003, 2004); 13 = Gröbern (Litt 1994; Walkling & Coope 1996; Kühl & Litt 2003; Kühl *et al.* 2007) (Klotz *et al.* 2003).

For palynological processing, 1 cm^3 was used per sample, and *Lycopodium* tablets were added for estimation of pollen concentrations prior to chemical treatment (Stockmarr 1971). Sediments were processed in 10% NaOH following Eisele *et al.* (1994). Residues were embedded in glycerine jelly, mounted on microscope slides and analysed with a Carl Zeiss Axio Scope A1® microscope (400–1000× magnification) at the Institute of Earth Sciences, Heidelberg University.

Loss on ignition (LOI) analysis

The organic-matter content of the sediment was measured in 89 samples between 888 and 794 cm core depth using 0.5–2 g of sediment per sample. The percentage of organic matter in each sample was determined following loss on ignition (LOI) at 550 °C following Heiri *et al.* (2001). LOI was conducted at the Department of Environmental Science, University of Basel.

Chironomid sample preparation and analysis

A total of 94 chironomid samples were taken every 1 cm along the sediment core between absolute sediment depths of 888 and 794 cm. The volume of sediment used ranged between 1 and 6 cm^3. For samples taken below and including 855 cm there was no chemical pretreatment, since the sediments could be sieved easily using water only. However, samples from 858 cm and above were heated in 10% KOH for 15 min at 85 °C due to processing difficulties (see below). All samples were sieved at 100 and 200 μm, and chironomid head capsules as well as other chitinous aquatic invertebrate remains were picked from a Bogorov tray under a stereomicroscope (30–50× magnification). Samples were dried and mounted in Euparal before identification at 40–400× magnification using a compound microscope. A minimum head count of 80 was aimed for to ensure that more than the recommended 45 head capsules were found per

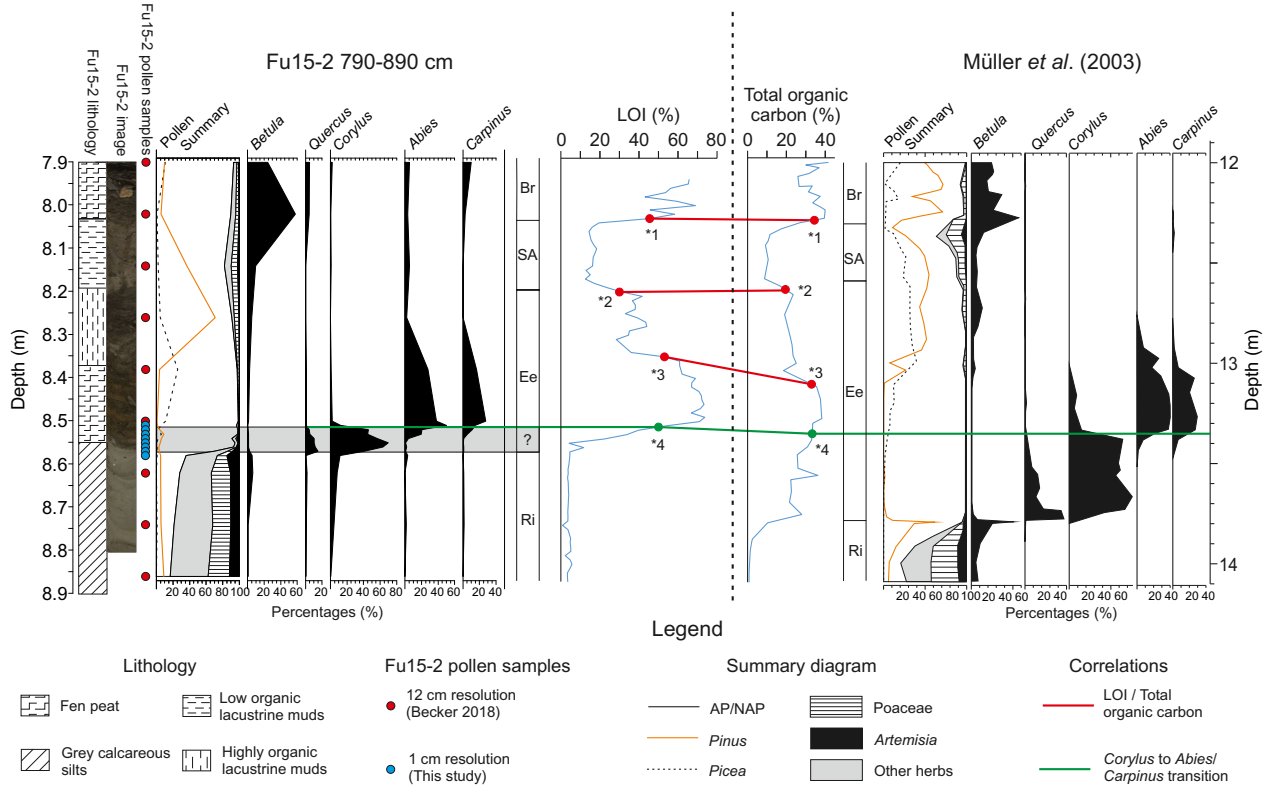

Fig. 2. Correlations between the Fu15-2 core and the published data of Müller *et al.* (2003), also from Füramoos. The red lines labelled *1, *2 and *3 are correlations based on changes in LOI (this study) and total organic carbon % (Müller *et al.* 2003). The green line labelled *4 is a correlation based on the palynostratigraphical transition from *Corylus*-dominated to *Abies*/*Carpinus*-dominated pollen assemblages. All four points were used to anchor the Fu15-2 core within the chronology of Müller *et al.* (2003) from Füramoos. The depths of pollen samples taken at 12-cm resolution by Becker (2018) are identified by red circles and the depths of the eight new pollen samples taken in this study are shown as blue circles. A sediment section of uncertain age in the Fu15-2 core, probably influenced by a hiatus, is displayed as a grey horizontal bar between 857–855 and 851.5 cm (see Discussion). Note that the interface between different lithological units at 857–855 cm is not perfectly horizontal. This resulted in a slight (1–2 cm) offset between major variations in organic matter, chironomid and pollen assemblages associated with this lithological transition, since these were sampled in different sides of the core (see Discussion). Ri = Rissian glacial; Ee = Eemian; SA = Stadial A; Br = Brörup.

sample (Heiri & Lotter 2001). Head capsules with a complete mentum or greater than half a mentum were counted as one specimen, head capsules with half a mentum were counted as half a specimen and head capsules with less than half a mentum were disregarded. Furthermore, other invertebrate remains including remains from *Daphnia*, Sialidae, Ceratopogonidae, mites, Ephemeroptera, Trichoptera and Plecoptera in addition to *Plumatella* resting cysts were mounted and identified. Characeae oogonia were also enumerated.

Chironomid identification

Chironomid identification followed Wiederholm (1983), Schmid (1993), Brooks *et al.* (2007) and Andersen *et al.* (2013). Specimens that could only be identified to low taxonomic resolution were excluded from further analysis. Samples consisting of peat were difficult to process (see below) and resulted in a relatively large number of mounted *Tanytarsus* specimens with damaged or missing antennal pedestals. In these sections head capsules belonging to specimens identified as *Tanytarsus* were assigned to the category of *Tanytarsus mendax-type,* since this was the only abundant *Tanytarsus* morphotype present in these samples. The descriptions of Solhøy (2001) and Haas (1994) were used to identify oribatid mites and Characeae oogonia, respectively. *Plumatella* statoblasts and *Daphnia* ephippia were identified based on Francis (2001) and Vandekerkhove *et al.* (2004). A reference collection of mounted modern specimens at Geoecology, University of Basel, was used to identify larval mandibles and head capsules of Sialidae, Ceratopogonidae, Ephemeroptera, Trichoptera and Plecoptera.

Chironomid-based temperature reconstruction

The Swiss-Norwegian calibration data set and inference model from Heiri *et al.* (2011) was used to develop quantitative July air temperature estimates based on fossil chironomid assemblages. The data set describes the

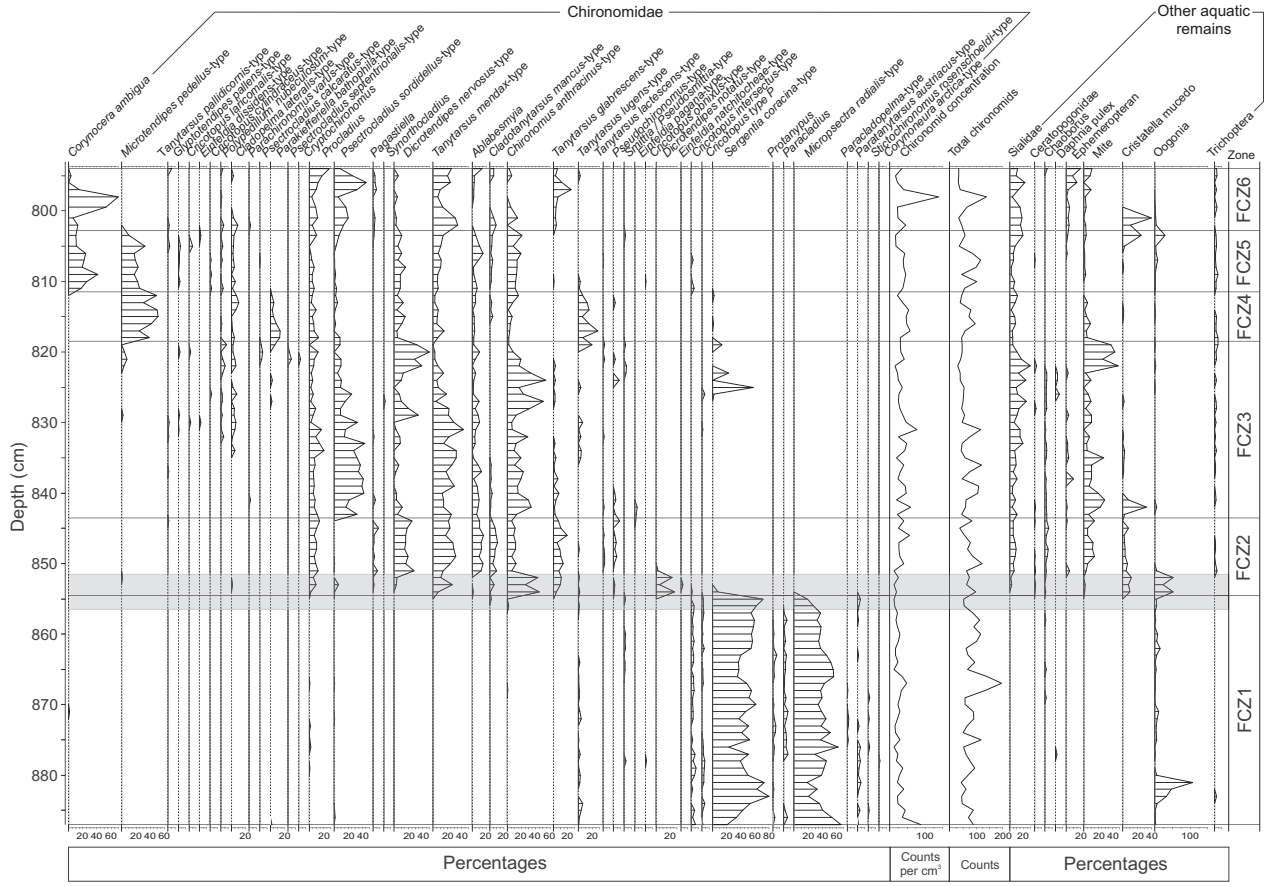

Fig. 3. Distribution of chironomids in the Fu15-2 790–890 cm core segment of the Füramoos record. Chironomid remains are displayed as percentages of total identified chironomids. Other aquatic remains are displayed as percentages relative to total chironomids including those that were not identified at higher taxonomic resolution. Chironomid zones were determined using CONISS. Chironomid types are ordered according to abundance weighted average depth of occurrence, with types more abundant at the top of the core displayed on the left and those more abundant at the bottom displayed on the right. All identified chironomid taxa from the core segment are shown. A sediment section of uncertain age probably influenced by a hiatus is displayed as a grey horizontal bar between 855 and 851.5 cm (see Discussion).

distribution data of 154 chironomid taxa from 274 lakes in Switzerland and Norway across a mean July air temperature gradient of 3.5–18.4 °C. A temperature reconstruction was produced using a two-component weighted averaging partial least squares model (WAPLS; ter Braak & Juggins 1993; ter Braak *et al*. 1993). To produce the reconstruction some Füramoos samples needed to be combined to achieve higher chironomid counts (see below and Fig. S1). The model used in this study had a root mean square error of prediction (RMSEP) of 1.41 and an r^2 of 0.90 between predicted and observed temperatures (estimates based on 9999 bootstrapping cycles). The chironomid samples in the record were identified to a higher resolution than the Swiss-Norwegian training set (Heiri *et al*. 2011) and therefore some of the original 42 types were aggregated to match the training set resolution. These were (training set resolution: Fu15-2 core resolution) *Einfeldia*: *Einfeldia dissidens-type* and *Einfeldia natchitocheae-type; Dicrotendipes: Dicrotendipes nervosus-type* and *Dicrotendipes notatus-type; Cricotopus* 292: *Cricotopus laricomalis-type* and *Cricotopus intersectus-type.* Furthermore, one type, i.e. *Psectrocladius calcaratus-type,* was not included in the calibration data set, resulting in 38 types that formed the basis for chironomid-inferred temperature estimates.

Samples were compared with the modern calibration data using squared chi-square distance to assess whether chironomid assemblages had either 'no close' or 'no good' modern analogues in the calibration data set. The 2nd and 5th percentiles of all distances in the modern calibration data set were set as thresholds for identifying subfossil samples with 'no close' or 'no good' modern analogues, respectively (Birks *et al*. 1990; Tóth *et al*. 2015). Goodness of fit statistics were calculated following Birks *et al*. (1990) by first conducting a canonical correspondence analysis (CCA) of the Swiss-Norwegian training set data with mean July air temperature set as the only constraining variable. The fossil data were analysed as passive samples. Samples with a 'poor' or 'very poor'

fit with temperature were identified by using the 90th and 95th percentile of residual distances of the modern calibration data set samples to axis 1, respectively (Birks *et al*. 1990; Tóth *et al*. 2015). Bootstrapping with 9999 cycles was used to calculate sample specific estimated standard errors of prediction for reconstructed temperatures (Birks *et al*. 1990). Rare taxa (N2 < 5 in the calibration data set; Heiri *et al*. 2003) and taxa absent from the training set were also calculated. The CCA was produced using CANOCO 5 (ter Braak & Smilauer 2018) and analogue statistics were calculated using the program C2 Version 1.7.7 (Juggins 2007). All analyses were based on square root transformed percentages.

Zonation and ordination analysis

Zones in the chironomid record were determined using the clustering algorithm CONISS (Grimm 1987) and a broken stick model (Bennett 1996) was used to test them for statistical significance. These analyses were performed using the *Rioja* (Juggins 2017) package on R studio version 1.1.463 (R Studio Team 2015). A detrended correspondence analysis (DCA) was calculated in CANOCO 5.1 (Šmilauer & Lepš 2014) to summarize major changes in the chironomid assemblage. Both analyses were conducted following sample aggregation and were calculated based on square root transformed percentages.

Results

LOI and organic matter content

The organic-matter content of Rissian sediments in the Fu15 core (887–855 cm) ranges between 0.8 and 5.7% (Fig. 2). Between 855 and 850 cm, there is an abrupt increase in organic-matter content from within a range of 0.8–5.7 to 71%. The organic matter reaches a peak of 74% at 849 cm before declining to 28–44% in the interval 835–820 cm. Low LOI values (12.5–19.5%) characterize the interval 819–804 cm. Further upcore, LOI values increase sharply to 43–69% in the interval from 803 to 794 cm.

Pollen analysis

The eight pollen samples processed for this study between 857 and 851 cm core depth show an abrupt transition from non-arboreal pollen (NAP) dominance to *Corylus* dominance at 857 cm (Fig. 2). Together with the information from the previously available samples of Becker (2018) from the same core section, the samples show steppe tundra in the Rissian glacial interval (890–858 cm) identified by high non-arboreal pollen (NAP) percentages of 65–80% associated with *Artemisia* abundances of 10–15%. However, the samples of Becker (2018) apparently show smearing of *Corylus* into the Rissian sediments below 857 cm, which does not make sense climatologically (*Corylus* is a warm-adapted tree species) and suggests some minor downward contamination of pollen samples in this record (Fig. 2). The abrupt transition at the onset of the Eemian sediments in the core segment at 857 cm shows arboreal pollen percentages rising to 90%, of which *Corylus* comprises 70% and *Quercus* 15% of the abundance. The initial stages of Eemian development at Füramoos, a *Pinus*/*Betula* peak followed by a peak in *Quercus* pollen (Müller *et al*. 2003; Fig. 2), are not observed in the Fu15-2 pollen sequence. Overall the pollen results in these intervals suggest some of the original sedimentation is missing and that the pollen stratigraphy may be influenced to some extent by vertical pollen transport in the latest Rissian samples. The exact chronological positions of these sections therefore remain uncertain and poorly constrained by the available stratigraphical data (see below). At 851.5 cm *Corylus* and *Quercus* are replaced by *Abies* and *Carpinus*, which increase to values of 50 and 27%, respectively. At 826 cm *Abies* declines to 5% abundance, and *Carpinus* disappears from the record with *Pinus* abundances increasing to 70%. During Stadial A, at 814 cm there is an increase in NAP to 18% coinciding with a decrease in *Pinus* from 70% in the Eemian to 36%. *Pinus* abundances decline further to 10% in the Brörup interstadial coinciding with maximum abundances of *Betula* of 67%.

The Füramoos chironomid record

Chironomid counts range from 26 to 193 head capsules per sample. Samples were aggregated based on chironomid head capsule counts to >30; >40 and >45 head capsules, 45 being the minimum number recommended for statistical analysis of fossil chironomid assemblages (Heiri & Lotter 2001). This produced three records with a total of 92, 84 and 82 samples per record, respectively. All three aggregated records were then used to perform temperature reconstructions and assess the differences between the reconstructed values (Fig. S1). The differences between the three records were minimal and therefore we continued this study using a minimum head capsule count of 30 and a total of 92 chironomid samples for all further analysis and presentation. CONISS zonation of the chironomid record identified five statistically significant breaks in the chironomid assemblage, resulting in six chironomid zones, i.e. Füramoos Chironomid Zone (FCZ) 1 through 6.

Zone FCZ1 (884.5–854.5 cm) is dominated by *Micropsectra radialis-type* and *Sergentia coracina-type.* Subdominant taxa include *Paracladius*, *Cricotopus* type P, *Cricotopus intersectus-type, Paratanytarsus austriacus-type, Tanytarsus lugens-type* and *Protanypus.* Zone FCZ2 (854.5–843.5 cm) begins with a drastic change in chironomid assemblages, *Micropsectra radialis-type* and *Sergentia coracina-type* disappear, and there is an

increase in chironomid-type diversity. *Tanytarsus glabrescens-type, Tanytarsus mendax-type* and *Procladius* dominate throughout the zone, although there are distinct changes in chironomid types within it. *Chironomus anthracinus-type* and *Dicrotendipes notatus-type* dominate initially before being replaced by *Cladotanytarsus mancus-type, Dicrotendipes nervosus-type* and *Ablabesmyia*. Within zone FCZ3 (843.5–818.5 cm) *Dicrotendipes nervosus-type* is replaced by *Psectrocladius sordidellus-type. Cladotanytarsus mancus-type* and *Tanytarsus glabrescens*-type initially decrease in abundance at the onset of FCZ3, and disappear later in the zone, while other taxa that were dominant in FCZ2 persist into FCZ3 and continue to dominate, including *Tanytarsus mendax-type, Chironomus anthracinus-type, Ablabesmyia* and *Procladius*. Zone FCZ4 (818.5–811.5 cm) begins with an increase in *Microtendipes pedellus-type* as well as *Tanytarsus lugens-type* and *Parakiefferiella*. The abundance of oribatid mites also decreases markedly from a maximum late in FCZ3. In zone FCZ5 (811.5–802.5 cm), *Tanytarsus lugens-type* and *Parakiefferiella bathophila-type* disappear and are replaced with *Corynocera ambigua*, while *Microtendipes pedellus-type* decreases in abundance. In zone FCZ6 (802.5–794 cm), *Microtendipes pedellus-type* disappears, and there is a strong increase in *Procladius*, *Psectrocladius sordidellus-type* and *Tanytarsus mendax-type. Tanytarsus glabrescens-type* also returns. There is a short, distinct increase in *Corynocera ambigua* percentages within zone FCZ6, with this type dominating the assemblages with abundances between 70 and 77%.

Chironomid-inferred July air temperature and ordination results

Chironomid-inferred temperatures show very little change within zone FCZ1 fluctuating around 8 °C within a range of 7–9 °C (Fig. 3). The onset of zone FCZ2 displays a marked and abrupt increase in temperature reaching 14 °C and increasing to 15–16 °C midway through the zone. Later, within FCZ3, there are distinct fluctuations in temperature but inferred temperatures display a general cooling trend across the zone with peak temperatures of 14 °C and minima of 12 °C. After the final cooling in FCZ3, temperatures remain at ~12.5 °C (range: 11–13 °C) within zones FCZ4 and 5. FCZ6 is characterized by a temperature decrease to ~10.5 °C and finally an increase to ~13 °C at the end of the zone.

DCA Axes 1 and 2 explain 29.7 and 7.5% of the variance in the chironomid record with axis lengths of 4.2 and 1.9 SD, respectively. Neither Axis 1 nor 2 varies within FCZ1 but both change markedly at the interface between FCZ1 and 2, DCA axis 1 decreasing from 4 to 0 SD and Axis 2 increasing from 0.5 to 1.9 SD. Axis 1 values remain low in FCZ2 and Axis 2 values decrease slightly after the initial peak. Axis 1 values exhibit signs of gradual increase beginning in FCZ3 culminating in a fluctuating interval resulting from the re-emergence of *Sergentia coracina-type* at the end of the zone, while Axis 2 increases during the same interval. Axis 1 values decrease into FCZ4, while Axis 2 remains low after the decrease at the end of FCZ3. DCA Axis 1 values decrease throughout FCZ5 and remain at ~0.2–0.4 SD. Axis 2 values decrease from FCZ4 into FCZ5 and generally increase in FCZ6.

Modern-analogue statistics suggest that no samples in the record have 'no good' modern analogue and only some samples, mainly between 826–820 and 808–798 cm have 'no close' modern analogue (Fig. 4). Most samples also have a good fit with temperature (Fig. 4) although the interval 798–796 cm is a notable exception with a 'very poor' fit with temperature. Taxa that were rare in the training set never exceed 3.5%, and only two samples contain types (*Psectrocladius calcaratus-type)* not included in the training set reaching a maximum of 4.8%.

Discussion

Correlations to earlier Füramoos records

The results of the LOI and pollen analyses allow correlation of the Fu15-2 core to the earlier total organic carbon and pollen records of Müller *et al*. (2003) who have previously described the lithology of the Füramoos palaeolake. The percentages of total organic carbon from Müller *et al*. (2003) are consistently lower than LOI as the latter measures total organic matter (rather than organic carbon) percentages. Four tie points were used to correlate the Fu15-2 core with the record of Müller *et al*. (2003) shown in Fig. 2 (*1, *2, *3 and *4). Tie points *1, *2 and *3 are based on large changes in organic carbon/organic matter (LOI) in the sediment samples and are supported by the available pollen data. Tie point *1 represents the beginning of the Brörup interstadial and is based on increasing LOI values following the low values during Stadial A, a transition that is associated with Brörup afforestation. Tie point *2 represents the beginning of Stadial A, is based on decreasing LOI values following the late Eemian and is associated with the onset of forest opening. Tie point *3 occurs at the transition from the mid-Eemian to late Eemian and is characterized by decreasing organic matter associated with the transition from *Abies*/*Carpinus* forest to *Pinus*/*Picea* forest. Tie point *4 is based on palynostratigraphy and ties the transition of the *Corylus*-dominated to *Abies*/*Carpinus*-dominated pollen assemblages in the Fu15-2 core to the record of Müller *et al*. (2003). All tie points were used in correlation and dating. The age estimates for tie points are *1 (104.5 ka), *2 (110 ka), *3 (118.8 ka) and *4 (125 ka) based on the Müller *et al*. (2003) chronology. For discussion and plotting a linear interpolation was used between the points to derive approximate age estimates for the interval from the mid-Eemian to end of Stadial A.

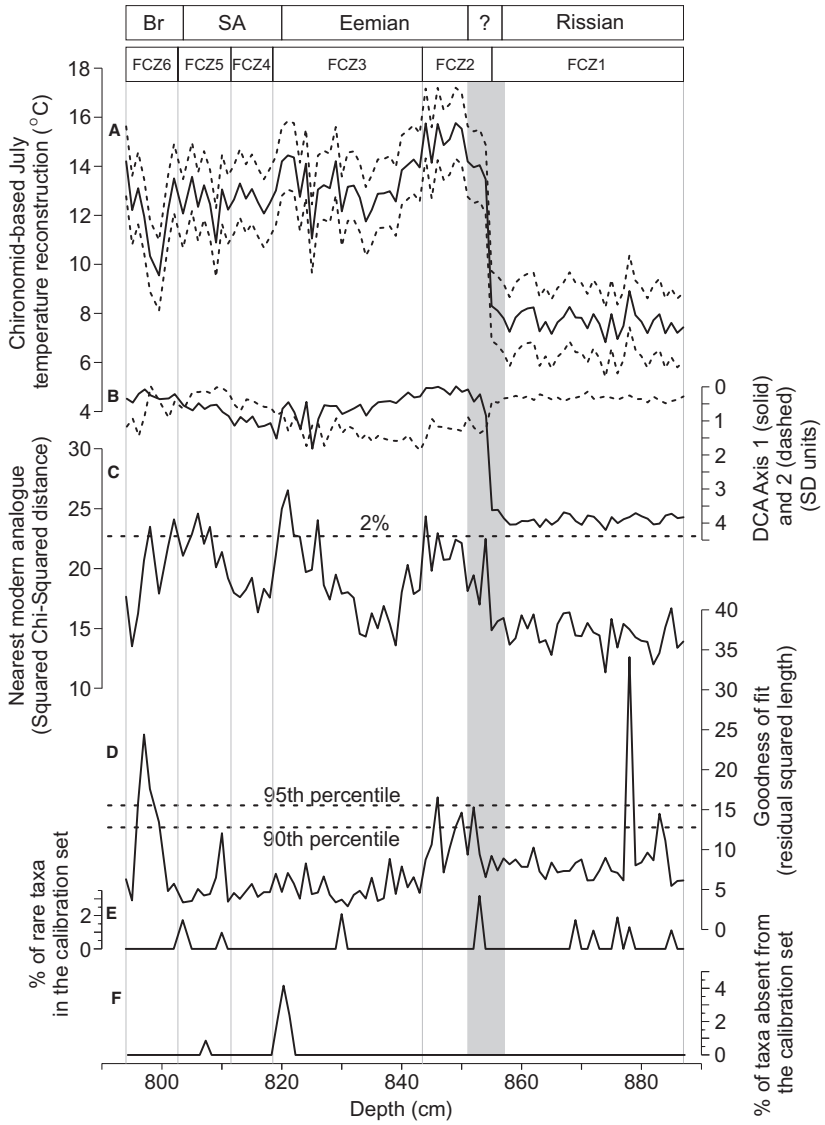

Fig. 4. Chironomid-inferred July air temperatures, ordination results and reconstruction diagnostic statistics based on the Fu15-2 chironomid record. A. Chironomid-inferred July air temperatures (solid line) and associated error estimates (dashed lines). B. DCA Axis 1 (solid line) and Axis 2 (dashed line) on reversed axis. C. Distance to nearest modern analogue in the calibration data set (squared chi squared distance). The threshold for identifying no close (2%) analogue is indicated by the dashed horizontal line following Tóth *et al.* (2015), the threshold for identifying samples with no good analogues (5%) is not shown since all samples had good analogues. D. Goodness of fit statistics with thresholds for 'poor fit' or 'very poor fit' identified as the 90th and 95th percentiles, respectively (dashed lines). E. Percentage of fossil taxa that are rare in the Swiss-Norwegian training set. F. Percentage of fossil taxa that are absent from the Swiss-Norwegian training set. The grey bar represents the chronologically poorly constrained sediment interval that probably contains a hiatus (see Discussion). SA = Stadial A; Br = Brörup.

The Rissian sediments below the chronologically uncertain interval at the Rissian to Eemian transition (897–855 cm) remain temporally less well constrained than the sections from the mid-Eemian to Stadial A, although their Rissian age is unequivocal (Müller *et al.* 2003). The ages of the sediments above tie point *1 (803–794 cm core depth) are also poorly constrained but unequivocally from the Brörup interstadial.

Sediments in the interval 851 to 855–857 cm of core segment Fu15-2 cannot be reliably correlated with the earlier record of Müller *et al.* (2003). A comparison of the LOI/organic matter and pollen records (Fig. 2) strongly suggests that sediment sections are missing in Fu15-2 at the Rissian to Eemian transition and in the earliest Eemian, as the gradual increase in LOI/organic matter apparent in the Müller *et al.* (2003) record is absent together with important features in the pollen record such as the initial afforestation by *Betula* and *Pinus* or the subsequent interval of *Quercus* dominance prior to the interval of *Corylus* dominance. Instead, in the Fu15-2 core there is an immediate transition from high percentages in NAP in the Late Rissian to high *Corylus*

dominance. The lithology of Fu15-2 also suggests an unexpectedly abrupt change in sediment composition at 855 cm with a transition from grey calcareous muds to fen peat (lithology and core image; Fig. 2). Available evidence therefore suggests that the oldest sediments in Fu15-2 are of late Rissian age, with a major hiatus and missing sediments characterizing the Rissian to Eemian transition as well as large parts of the early Eemian. The early to mid-Eemian transition characterized by the *Corylus* to *Abies*/*Carpinus* transition is well represented in the pollen record and provides a reliable stratigraphical marker. However, the age and stratigraphical position of the Eemian sediments older than this transition remain uncertain (grey bar in Figs 2, 3 and 4), also because the LOI record does not show the plateau of intermediate organic matter values reported by Müller *et al*. (2003) for the early Eemian. We therefore consider these sediments poorly constrained stratigraphically and of uncertain age and do not interpret chironomid-inferred temperatures from this section of the Fu15-2 record.

The interpretation of the Rissian to Eemian transition and early Eemian in the Fu15-2 core is further complicated by a slight (~1–2 cm) offset between variations in pollen assemblages on one hand and the LOI and chironomid assemblages on the other. This is a result of pollen samples being taken from the side of the sediment core while chironomid and LOI samples were taken from the centre. For the majority of the sequence this has not adversely affected interpretations. However where there are high resolution pollen data between 857 to 851 cm, the boundary between the Rissian and Eemian sediments, which we interpret as a hiatus, is not perfectly horizontal (Fig. 2) and has led to a slight offset between the records. As a consequence, the rapid transition between cold stenothermic chironomid assemblages associated with the Eemian to more temperate taxa is apparent at 855 cm, as is the initial LOI increase. In contrast, the initial increase in *Corylus* pollen occurs at 857 cm even though this represents the same environmental transition in the record.

Processing and analysis of strongly compacted samples

Fu15-2 core sections 854–818 and 803–794 cm are characterized by fen peat deposited in limnic environments and consist of strongly compacted sediment with moderate to high organic-matter contents. Extracting chironomid head capsules from them was challenging and very time consuming. The sediments in these sections were very hard, appearing homogenous in the section 854–818 cm, and having a hard structure consisting of platelets of organic matter that were remarkably resistant to bending or breaking in section 803–794 cm. A month of submersion in 4 °C water yielded no changes to the consistency of sediments from either section. Breaking the samples into smaller pieces and then immersing them in 10% KOH at 85 °C for 15 min (Brooks *et al*. 2007) loosened the sediment matrix and allowed the material to be more readily separated. Immersing a single large sediment sample, >2 cm^3, into the 10% KOH solution overnight at room temperature only softened the material on the exterior while the internal sediments were unaffected. Sieving the treated sediments removed very little material, only breaking the sediment into smaller pieces and expanding the sediment volume as it became less compact, similarly to what was observed by Behre *et al*. (2005) in a beetle assemblage reconstruction from peat sediments from Oerel, northern Germany. Most chironomid specimens in samples from sections 854–818 and 803–794 cm were trapped in organic material >200 μm in size and needed to be manually separated from the sediment matrix for mounting (examples in Fig. 5). Many of the specimens from sections 854–818 and 803–794 cm were damaged as a result of sediment processing, e.g. torn in two with parts critical for identification missing. No further or harsher pretreatments were used as these would likely have resulted in further damage to the remains.

Within the sediment sections 854–818 and 803–794 cm, many Tanytarsini were missing antennal pedestals and mandibles as they were torn off during mounting. Both the antennal pedestals and mandibles are important identification features for the Tanytarsini, needed to achieve identification at a higher taxonomic resolution (Brooks *et al*. 2007). For sections 854–818 and 803–794 cm, three *Tanytarsus* types were identified that could not be reliably identified to type resolution without the antennal pedestals/mandibles: *Tanytarsus mendax-type, Tanytarsus pallidicornis-type* and *Tanytarsus lactescens-type.* In this study, for the entire core, *Tanytarsus mendax-type* were consistently in far higher abundance than both the *Tanytarsus pallidicornis-type* and *Tanytarsus lactescens-type* head capsules. Furthermore, identified *Tanytarsus mendax-type* specimens were present in every sample in the 854–818 and 803–794 cm intervals whereas *Tanytarsus pallidicornis-type* and *Tanytarsus lactescens-type* only occurred intermittently. Therefore, for further analysis all unidentified *Tanytarsus* were reclassified as *Tanytarsus mendax-type* in these sections. Unidentified Tanytarsini that could not be clearly associated with *Tanytarsus* were not taken into account for further analysis.

Ecological interpretation by assemblage zone

Chironomid assemblages from zone FCZ1 indicate prevailing cold temperatures. *Micropsectra radialis-type* and *Sergentia coracina-type* are typical for cold, oligotrophic lakes in sub-arctic to arctic and sub-alpine to alpine environments (Heiri *et al*. 2011). The dominance of *Micropsectra radialis-type* (Fig. 2) also indicates highly oxygenated water (Brodersen *et al*. 2004) and an ultraoligo-/oligotrophic lake environment (Saether

1979; Brodersen & Anderson 2002; Brooks *et al*. 2007) with low productivity. Overall FCZ1 represents cold and oligotrophic conditions.

Many of the taxa present within the first part of zone FCZ2, such as *Dicrotendipes notatus-type, Chironomus anthracinus-type* and *Procladius* have wide thermal tolerances (Brooks *et al*. 2007; Luoto *et al*. 2019). *Dicrotendipes notatus-type, Chironomus anthracinus-type* and *Tanytarsus glabrescens-type* are dominant at the beginning of FCZ2 suggesting relatively warm conditions (Brooks *et al*. 2007; Heiri *et al*. 2011). At 851 cm core depth, *Dicrotendipes notatus-type* is

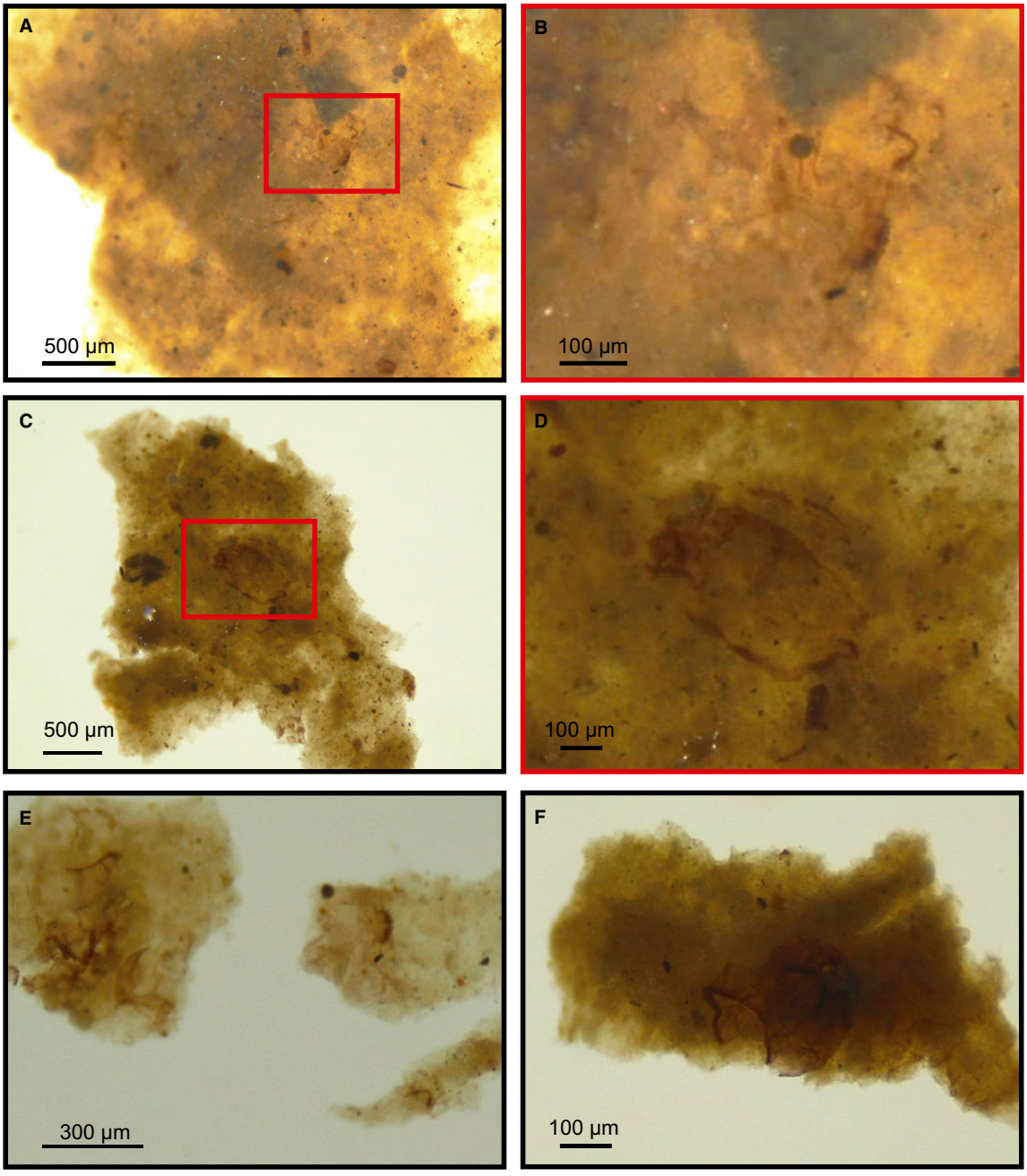

Fig. 5. Examples of chironomids embedded in highly compacted fine organic material (fen peat) under a stereomicroscope. A, B. (796 cm core depth). Overview (A) and detailed view (B) of a pair of chironomids trapped in a large piece of organic matter where B represents the area encompassed by the red box in A. C, D. (800 cm core depth). Overview (C) and detailed view (D) of a single chironomid trapped in a large piece of organic matter where D represents the area encompassed by the red box in C. E, F. (core depths 796 and 795 cm, respectively). Chironomids extracted from the compacted organic material and in need of cleaning. Note that the two chironomids on the right-hand side of E are the same specimens as displayed in A, B. All samples are from fen peat.

replaced by *Dicrotendipes nervosus-type* and the abundance of *Chironomus anthracinus-type* is reduced, at the same time as oribatid mites increase in the record. These changes are associated with abundance increases of *Cladotanytarsus mancus-type, Tanytarsus mendax-type* and *Tanytarsus glabrescens-type,* all of which are typical for temperate to warm lakes (Brundin 1949; Saether 1979; Brodin 1986; Brooks *et al*. 2007; Heiri *et al*. 2011). The presence of Sialidae throughout the zone suggests the presence of a shallow water environment near the coring site (Lemdahl 2000). Similarly, many of the chironomids in this zone (e.g. *Dicrotendipes nervosus-type* and *Dicrotendipes notatus*-type) are typical for littoral to sublittoral habitats (Walker *et al*. 1991; Millet *et al*. 2007). Overall FCZ2 is considered representative of a warm, productive lake.

The onset of zone FCZ3 is defined by a pronounced increase of *Psectrocladius sordidellus-type* and associated decrease of *Dicrotendipes nervosus-type.* Both *Psectrocladius sordidellus-type* and *Dicrotendipes nervosus-type* are associated with littoral to sublittoral habitats in temperate lakes (Brooks *et al*. 2007; Nazarova *et al*. 2017) and can occur in lakes across a wide temperature range although the thermal optimum of *Psectrocladius sordidellus-type* is slightly lower than *Dicrotendipes nervosus-type* (Heiri *et al*. 2011). Less pronounced changes include the decrease and almost complete removal of *Tanytarsus glabrescens-type* and *Cladotanytarsus mancus-type,* which supports a decrease in temperature as, while they are both able to occur in cool lakes, these taxa are generally considered to be thermophilic (Brundin 1949; Saether 1979; Brodin 1986; Brooks *et al*. 2007). In the upper section of FCZ3 there is an oscillation in the chironomid assemblage (between 829.5 and 818.5 cm) where *Tanytarsus mendax-type* and *Psectrocladius sordidellus-type* are replaced by *Dicrotendipes nervosus-type,* then by *Chironomus anthracinus-type* and finally, *Sergentia coracina-type* followed by a reversal to *Chironomus anthracinus-type* and *Dicrotendipes nervosus-type.* In a shallow lake environment this change in chironomid assemblages suggests cooling to a temperature minimum at 825 cm with maximum abundances of *Sergentia coracina*-type, which has a preference for cold water (Brooks & Birks 2000; Heiri & Lotter 2010; Heiri *et al*. 2011) followed by a warming. Alternatively, this change could suggest a deepening of the lake reaching a maximum depth at 825 cm followed by a subsequent shallowing. This is because while *Sergentia coracina-type* is a cold stenotherm (Brooks *et al*. 2007), it is able to persist in temperate lakes in the cool waters beneath a thermocline where there is sufficient oxygen (Hofmann 2001; Bolland *et al*. 2020). The lake level change scenario is supported by the increasing abundance of oribatid mites following the *Sergentia coracina-type* peak at 826 cm, which can indicate shallow littoral environments (de la Riva-Caballero *et al*. 2010; Heggen *et al*. 2012). Overall, FCZ3 appears to represent a cooler and less productive lake than FCZ2 that culminates in either a temperature or lake level oscillation.

There is a pronounced change at the onset of zone FCZ4 with *Microtendipes pedellus-type* replacing *Dicrotendipes nervosus*-type, as well an increase in *Tanytarsus lugens-type* and *Parakiefferiella bathophila-type. Microtendipes pedellus-type* and *Tanytarsus lugens-type* are typical for cooler lakes (Heiri *et al*. 2011) with *Tanytarsus lugens-type* also indicating a well-oxygenated and more oligotrophic system (Frey 1988). The low organic matter content in FCZ4 (<20%) supports the interpretation of a less productive environment and may have promoted the dominance of *Microtendipes pedellus-type* (McGarrigle 1980; Millet *et al*. 2007), a taxon that has a preference for sediments with low organic content and a coarse grain size (McGarrigle 1980). Overall FCZ4 indicates a cool and relatively unproductive lake.

In zone FCZ5 there is an increase in *Corynocera ambigua* and *Chironomus anthracinus-type,* an associated decline in *Microtendipes pedellus-type* and the disappearance of *Tanytarsus lugens*-type. *Chironomus anthracinus-type* can occur over a broad temperature range of 8–16 °C (Heiri *et al*. 2011) and the most telling indication of temperature change in FCZ5 is the disappearance of the cold stenotherm *Tanytarsus lugens-type,* which implies climatic warming relative to FCZ4 (Heiri *et al*. 2011). Overall the chironomid assemblage from FCZ5 indicates a cool lake with low productivity that may have been warmer than in FCZ4.

The onset of zone FCZ6 is characterized by a disappearance of *Microtendipes pedellus-type,* which, in this record, is restricted to sediments with low organic-matter contents. This may indicate that the decline was a response to increasing LOI associated with FCZ6 as *Microtendipes pedellus-type* has a preference for sediment with low organic content and coarse grain size (McGarrigle 1980). The increase in LOI suggests an increase in productivity and the reoccurrence of *Tanytarsus glabrescens-type,* which reaches up to 25% in FCZ6, supports an increase in temperatures as it is generally considered to be thermophilic (Brooks *et al*. 2007; Heiri *et al*. 2011). Furthermore it is likely that there was a large littoral to sublittoral area in the lake indicated by the high abundances of *Psectrocladius sordidellus-type* (Brooks *et al*. 2007; Nazarova *et al*. 2017). Overall, the chironomid assemblage indicates a response to increasing temperatures and increasing productivity in the lake.

Temperature reconstruction, vegetation change and organic-matter content

The new chironomid-inferred temperature record from Füramoos reconstructs July air temperatures in a range of 6.6–16 °C from the Rissian, mid- and Late Eemian, Stadial A and the first section of the Brörup interstadial. Most samples have both a good fit with temperature and close modern analogues (Fig. 4). Previous analysis of

chironomid samples at Füramoos for the Last Glacial Period (*c*. 99–46 ka) indicated that most chironomid assemblages had either 'no close' or 'no good' analogues (Bolland *et al*. 2021). Therefore the chironomid assemblages presented here for the Late Rissian, Eemian, Stadial A and early Brörup appear more similar to modern chironomid assemblages than chironomid assemblages from later intervals in the Last Glacial Period. Furthermore, the WAPLS regression model used to produce the July air temperature reconstruction typically handles non-analogue situations relatively well (Lotter *et al*. 1999), lending more confidence to those few samples displayed here that have 'no close' modern analogue. The ecological analysis of chironomid and other invertebrate assemblages indicated moderate lake level change that could have influenced the temperature reconstruction. Such lake level changes and associated effects such as variations in thermocline development, oxygen availability and food quantity can alter chironomid assemblage compositions in lakes (Brooks *et al*. 2007; Engels & Cwynar 2011; Eggermont & Heiri 2012). However, the Swiss-Norwegian training set is composed of 274 lakes with a depth range of 0.9–85 m (Heiri & Lotter 2010; Heiri *et al*. 2011). Therefore any influence that changes in water depth have on temperature reconstruction can be expected to be incorporated into the model prediction error and the sample-specific estimated standard errors of prediction of 1.6–1.8 °C. Fen peat in the intervals 855–837 and 803–790 cm contains abundant remains of fully aquatic chironomid and other invertebrate remains (Fig. 3). Therefore despite the changing wetland habitat, the sediments were clearly deposited in open water conditions that are well represented by chironomid assemblages in the Swiss-Norwegian training set and do not indicate that the coring site dried out in this interval, as in such situations open water taxa would disappear and semi-terrestrial to terrestrial chironomid and invertebrate remains would be expected to increase in abundance (see, e.g. Bolland *et al*. 2021).

In the late Rissian glacial period (887–857 cm) the chironomid-based temperature reconstruction indicates mean July air temperatures of 7–9 °C. The landscape around the lake was an open tundra environment as indicated both by the correlation of our record to the sediment core of Müller *et al*. (2003) and by the pollen samples available for this sediment section (Fig. 2). The lower July air temperature limit for tree growth is presently around 8.5–9.5 °C in central Europe (Landolt 2003), and therefore the reconstructed temperatures agree with the persistence of open tundra. Similarly, the low organic-matter content of these sediments agrees with the interpretation of a lake situated in cold climate conditions with low in-lake productivity. However, the exact age of these late Rissian sediments is difficult to constrain based on the available stratigraphical data.

Following the hiatus at 855 cm the sediments in Fu15-2 are characterized by fen peat and are dominated by *Corylus* pollen until 851.5 cm. *Corylus* dominance in the early Eemian is observed on the German alpine foreland (Müller 2000; Müller *et al*. 2003), eastern France (de Beaulieu & Reille 1984, 1992a, b; Reille & de Beaulieu 1990) and northern Germany (e.g. Litt 1994); however, the exact stratigraphical position of this entire interval is not well constrained in Fu15-2 due to obviously missing sediments in this section and uncertainties in correlating the sediments with the earlier pollen record of Müller *et al*. (2003). The early Eemian has been reported to be the warmest section in the entire interglacial interval for central Europe (e.g. Zagwijn 1996) and therefore it seems unusual that the chironomid-inferred temperatures were lower in those samples from the early Eemian (14 °C maximum) when compared to the mid-Eemian (15.5 °C maximum; Fig. 5). Also, the early Eemian chironomid assemblages between 855 and 851 cm are not statistically different from those in the mid-Eemian (CONISS Zonation; Fig. 3) and a more pronounced assemblage shift would be expected if they originated from the distinctly warmer climatic conditions of the early Eemian. Finally, the organic matter content of these sediments also does not agree with the relatively high and constant values observed for the late early Eemian in the record of Müller *et al*. (2003). Without robust supporting evidence from a parallel core we have decided to omit samples between the depths of 857 to 851 cm from further analysis and not discuss reconstructed temperatures from the early Eemian in the Fu15-2 record.

The mid-Eemian occurs between 851–835 cm and is defined by *Abies* and *Carpinus* pollen dominance based on a comparison with Müller *et al*. (2003) who present a palynostratigraphical record from the same site. The inferred chironomid-based July air temperatures within this section decrease from 15–15.5 to 12–12.5 °C and are associated with the presence of pollen of the thermophilic tree genus *Carpinus*, which is a common feature of mid-Eemian pollen records in central Europe, e.g. at La Grande Pile (eastern France; Woillard 1978; de Beaulieu & Reille 1992a), Les Echets (eastern France; de Beaulieu & Reille 1984; Reille & de Beaulieu 1990b), Jammertal (southern Germany; Müller 2000; Müller *et al*. 2005) and Gröbern (northeastern Germany; Litt 1994). The Füramoos palaeolake was likely at its most productive state between the depths 851–835 cm during the mid-Eemian, indicated by its association with maximum organic-matter contents of 75%.

The pollen evidence from the Fu15-2 core documents the transition from the mid-Eemian into the late Eemian at 835 cm, which lasts until 819 cm. The mid- to late Eemian transition, identified as the transition from an *Abies* and *Carpinus* dominated pollen assemblage to a *Pinus* pollen dominated assemblage coincides with chironomid-inferred July air temperature decreasing to 12 °C (Fig. 5). This evidence implies that decreasing July

air temperatures may have contributed to the transition from *Abies* and *Carpinus* forests to *Pinus* and *Picea* forests in the late Eemian, as *Pinus* and *Picea* are typical for cool temperate to boreal forests (Beck *et al*. 2016; Caudullo *et al*. 2016; Durrant *et al*. 2016). Furthermore, organic matter content decreases from 60–75% in the mid-Eemian to 28–45% in the late Eemian (Fig. 2) suggesting that the lake became less productive. Late Eemian July temperatures vary between 12–14 °C, temperatures at which pollen assemblages dominated by *Abies* and *Carpinus* persisted in the mid-Eemian; however, neither the Fu15-2 pollen record nor the Müller *et al*. (2003) Füramoos pollen record indicates subsequent increases in *Abies* and *Carpinus* in the late Eemian. Therefore it seems that that environmental or climatic variables other than summer temperature prevented the reestablishment of more thermophilic tree taxa during the late Eemian.

Stadial A occurs in the interval from 819 to 803 cm in the Fu15-2 core and is associated with low organic matter content decreasing from 40% in the late Eemian to <20%. *Pinus* dominated forests opened, as indicated by an initial reduction in arboreal pollen to 90% that declines further to 65% in the later part of Stadial A (Müller *et al*. 2003; Fig. 6). Although the onset of Stadial A is associated with a decrease in chironomid-inferred July air temperature from 14 to 12.5 °C, suggesting that initial forest opening could have been driven in part by July air temperature, temperatures in Stadial A largely remain comparable to those of the late Eemian. Interestingly however, despite the similar temperatures inferred in the late Eemian and Stadial A there are completely different chironomid assemblages inferred for these two intervals and chironomid assemblage change at this transition therefore does not appear to be driven by changes in July air temperature. The chironomid assemblages of the late Eemian have a high proportion of *Chironomus anthracinus-type,* a taxon that has been reported to prefer softer and more organic sediments (McGarrigle 1980). In contrast, chironomid assemblages from Stadial A contain a high proportion of *Microtendipes pedellus-type,* which has been reported to have an ecological preference for less organic sediments with a higher grain size (McGarrigle 1980). The transition between the chironomid assemblages of the late Eemian and Stadial A is also associated with a transition from more organic sediments in the late Eemian (20–45%) to less organic sediments in Stadial A (13–20%), shown by both the sediment core image (Fig. 2) and the results of LOI analysis (Figs 2, 6). Therefore chironomid assemblages appear to have responded to changes in the sedimentary properties of the lake, while at the same time the chironomid based temperature reconstruction major changes in July air temperature. A similar result was also observed by Bolland *et al*. (2021), who show a transition from chironomid assemblages indicative of more organic lake sediments, to *Microtendipes pedellus-type* dominated assemblages in less organic sediments at the transition from the Brörup interstadial to Stadial B (*c*. 87 ka) at Füramoos. In both of these intervals forest opening appears to be associated with possibly increased erosion and clastic inputs into the lake and lower in-lake productivity, resulting in lower sedimentary organic matter contents and a subsequent change in chironomid assemblage. As chironomid-inferred temperatures during Stadial A remain similar to those in the late Eemian, this also implies that for Stadial A forest opening was not driven by summer air temperature change.

Sediment at 803–794 cm depth was deposited during the Brörup interstadial and organic matter content increases from <20% to a range of 45–70%. At the onset of the Brörup interstadial July air temperatures remain in the range of 12–14 °C, similar to the temperature range apparent in the chironomid-inferred temperature reconstruction for Stadial A. There is an initial increase of *Betula* pollen abundance at the onset of the Brörup to 58% followed by an increase in *Pinus* pollen to 70% indicating forest closing following Stadial A (Müller *et al*. 2003). As the reforestation during the Brörup is not associated with a July air temperature increase in our record it is likely that a climatic variable other than July air temperature was limiting afforestation during the Stadial A interval, and that variable was no longer limiting in the Brörup. There is a clear temperature decrease to 9.5–10 °C associated with sediment depths 799–797 cm in the Brörup sediments characterized by very high (>50%) abundances of *Corynocera ambigua*. This taxon was originally described as an indicator of cold temperatures (Luoto 2009) and has been shown to dominate in the cooler samples of the calibration data set used in the transfer function (Heiri *et al*. 2011). However, it has also been reported in lakes with relatively warm temperatures including eutrophied lowland lakes in Denmark (Brodersen & Lindegaard 1999) and warmer lakes in Russia (Nazarova *et al*. 2015), thus apparently having a wider thermal tolerance than originally thought (Brodersen & Lindegaard 1999). This temperature decrease should therefore be interpreted with caution unless further evidence becomes available supporting a short-term summer temperature cooling at Füramoos in the early Brörup.

Comparison with summer temperature reconstructions from central Europe based on biotic proxies

Rissian glaciation. – Our new chironomid-based temperature reconstruction from Füramoos yields late Rissian July air temperatures of 7–9 °C. These temperatures are consistent with the relatively narrow temperature range produced by beetle-based mean temperature of the warmest month reconstructions from La Grande Pile (8–12 °C; Ponel 1995). Zagwijn (1996) used 31 pollen records from across northwestern and central Europe to produce a pollen-based mean temperature of the warmest

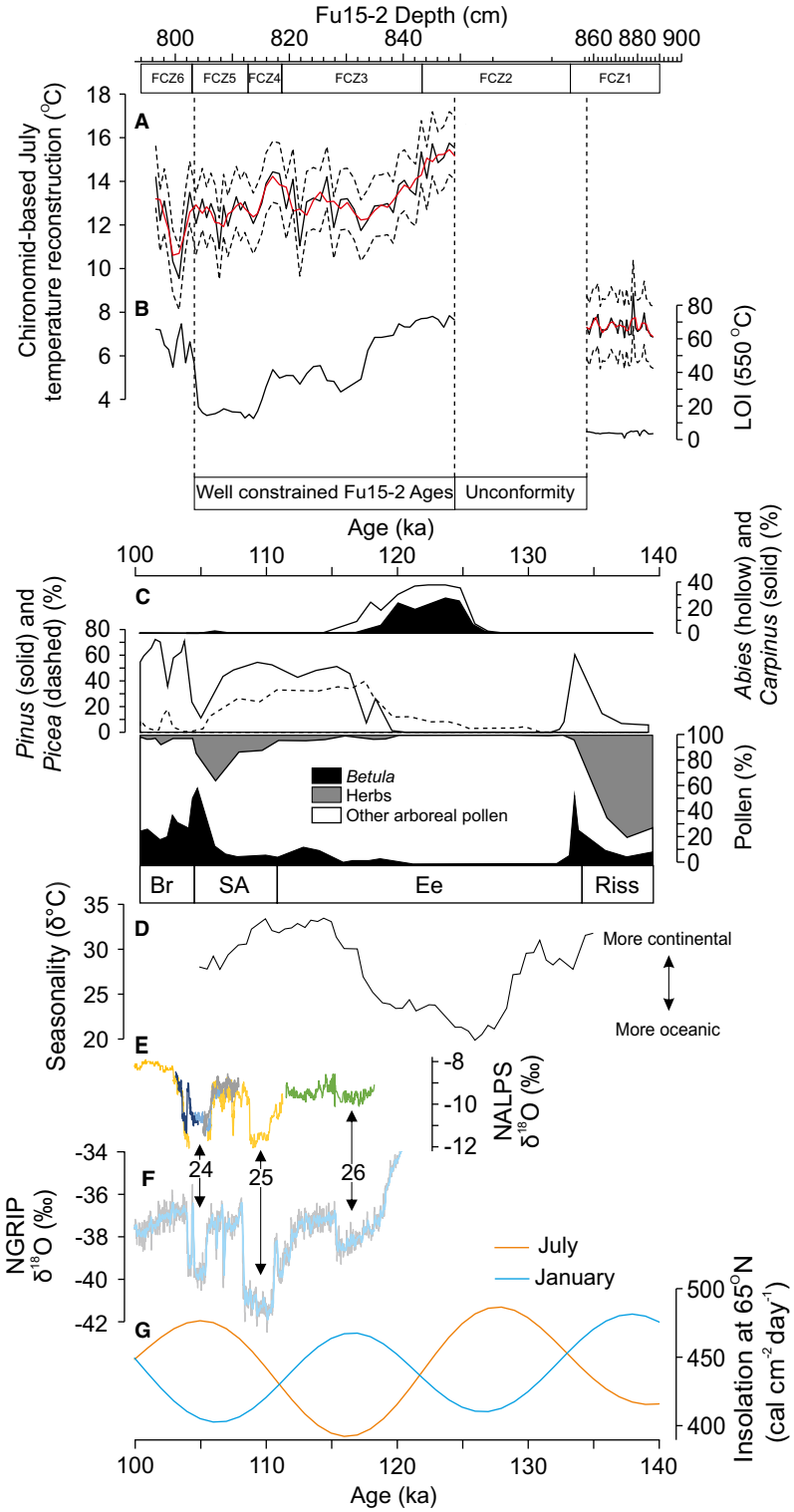

Fig. 6. A. Chironomid-inferred July air temperature reconstruction for Füramoos (black line) and associated error estimates (dashed black lines) and three sample running average (red line). B. LOI %. C. Selected pollen data from the Füramoos pollen record (Müller *et al.* 2003). *Abies* and *Carpinus* as well as *Pinus* and *Picea* are superimposed, and the summary graph of *Betula*, herbs and other arboreal pollen is stacked. D. Seasonality (temperature difference between warmest and coldest month) reconstructed based on 17 European pollen records, higher values indicate more continental climate (Brewer *et al.* 2008). E. NALPS $\delta^{18}O$ record (Boch *et al.* 2011; Moseley *et al.* 2020). F. GRIP $\delta^{18}O$ record on NGRIP chronology (Johnsen *et al.* 1997; Rasmussen *et al.* 2014). G. January and July insolation at 65°N (Berger & Loutre 1991). Numbered arrows indicate GS stages in the NALPS and GRIP records. Riss = Rissian glacial; Ee = Eemian; SA = Stadial A; Br = Brörup.

month estimate that suggests low temperatures of 10 °C prior to the onset of the Eemian Kühl & Litt (2003) indicate warmer Rissian temperatures of 13 °C at Gröbern, Germany, using pollen-based probable mean July temperatures, as do Müller *et al.* (2005) who estimate summer temperatures between 11–13.5 °C from Jammertal, southern Germany. The pollen-based reconstructions of Klotz *et al.* (2003) from sites across eastern France, the Swiss plateau and Germany generally indicate higher Rissian temperatures of the warmest month ranging between 10 and 22.5 °C with the exception of Beerenmösli, Switzerland, that has a Rissian temperature range of 5–17.5 °C. Furthermore the warmest temperature range presented by Klotz *et al.* (2003) for the late Rissian is from Füramoos, where a temperature range of 14–22.5 °C is presented in stark contrast to the 7–9 °C resulting from the new chironomid-based reconstruction.

The discrepancy between some of the late Rissian temperature reconstructions (Table 1) could be a result of how the different biotic proxies, used to develop the summer temperature reconstructions, respond to climatic changes. Chironomid assemblages in shallow lakes are closely related to summer temperature (Eggermont & Heiri 2012), but also protected from extreme winter temperature and precipitation changes so long as the lake they are in does not completely freeze or dry out (Lotter *et al.* 2012; Samartin *et al.* 2017). In contrast, the vegetation surrounding a lake is exposed to extreme winter temperatures and is more susceptible to changes in moisture and precipitation, and as such pollen can be more reliable for reconstructing January temperatures and precipitation than for July air temperature (Cheddadi *et al.* 1998). Discrepancies in the July air temperature estimations from parallel chironomid- and pollen-based reconstructions have also been identified and discussed by Lotter *et al.* (2012) in a study from Gerzensee, Switzerland, covering the Würmian Lateglacial. The disparities between the reconstructions were attributed to vegetation responding more strongly to changes in seasonality and precipitation and chironomid assemblages responding more strongly to summer temperature change.

Discrepancies such as the difference between the new late Rissian chironomid-based July air temperature estimates from Füramoos of 7–9 °C and the pollen-based temperature reconstruction of Klotz *et al.* (2003) of 14–22.5 °C, can also be evaluated by ecologically assessing the assemblages from which the reconstructions were developed. The chironomid assemblage in the Rissian Lateglacial was dominated by two chironomid morphotypes, *Micropsectra radialis-type* and *Sergentia coracina-type,* which, as discussed above, indicate a cold, oligotrophic lake, in line with the 7–9 °C July air temperature range produced by the transfer function in this study. The pollen assemblage used to produce the 14–22.5 °C mean temperature of the warmest month estimate for the Rissian Lateglacial (Klotz *et al.* 2003) was dominated by NAP (80% abundance) including an *Artemisia* abundance of 11% and Poaceae abundance of 32%. At other sites and based on other reconstruction methods this type of late Rissian vegetation has been considered to represent a cold steppic tundra (e.g. Guiot *et al.* 1989; Zagwijn 1996; Bińka & Nitychoruk 2001). It therefore appears that the reconstructions by Klotz *et al.* (2003) may have overestimated summer temperature values based on this pollen assemblage type. This example highlights the necessity of comparing a temperature reconstruction, or any other quantitative biotic proxy-based reconstruction, against the assemblage from which it was developed, and determining if it makes sense ecologically and in a broader palaeoecological or palaeoclimatological context (Birks *et al.* 2010).

Mid- and late Eemian. – Summer temperature reconstructions for the mid-Eemian from central Europe are very similar despite the different biotic proxies used. The chironomid record from Füramoos yields a July air temperature range of 12–16 °C for the mid-Eemian (*c.* 118–125 ka; Fig. 5). This temperature range is similar to the lower range of the estimates for mean temperature of the warmest month using beetle assemblages for La Grande Pile of 13–26 °C (Ponel 1995; Table 1) as well as pollen-based temperature reconstructions that produce temperature estimates from across central Europe indicating a summer temperature range of 14–19.5 °C (e.g. Kühl & Litt 2003; Kühl *et al.* 2007; Table 1). Summer temperature reconstructions for the late Eemian (*c.* 110–118 ka) are also similar for central European records produced with biotic proxies. The new chironomid-based July air temperature reconstructions from Füramoos indicate a temperature range of 12–14 °C for the late Eemian that is in good agreement with the lower range of summer temperature estimates for both beetle-based reconstructions that range from 11–25 °C (e.g. Ponel 1995) and pollen-based temperature reconstructions that range from 10–21.5 °C (e.g. Kühl & Litt 2003; Klotz *et al.* 2004; Table 1).

In general the proxy-based summer temperature reconstructions presented in Table 1 describe a decrease in temperature from the mid-Eemian to the late Eemian, and Field *et al.* (1994) further suggest a reduction in growing degree days (calculated relative to 5 °C) from the Eemian thermal optimum to the late Eemian in Bispingen (northern Germany) based on pollen data. While overall there is a clear decrease in the lower range of summer temperature estimates in all proxies, many of the upper limits of estimation from the pollen-based summer temperature reconstructions remain relatively warm, indicating thermal conditions uncharacteristic for boreal conifer forests (Kühl & Litt 2003; Klotz *et al.* 2004). Beetle-based temperature reconstructions produced with the mutual climatic range method containing many eurythermic species can produce very broad estimates of temperature. Behre *et al.* (2005) use a calibration method that narrows the temperature range produced from beetle-based mutual

Table 1. Summer temperature reconstructions from central Europe for the Rissian glacial, mid-Eemian, late Eemian, Stadial A and the Brörup based on biotic proxies. Mean July air temp. = mean July air temperature; MTW = mean temperature of the warmest month; TMAX = mean temperature of the warmest month; TMAXcal = calibrated mean values of the mean temperature of the warmest month; Summer temp = summer temperature. We do not compare early Eemian temperatures in this study, since this interval is not reliably represented in the Füramoos chironomid record. N/A represents intervals in which data are not available.

Author	Proxy	Site	MIS stage Stage name	5c Brörup	5d Stadial A	5e Late Eemian	5e Mid-Eemian	5e Early Eemian	6 Rissian
This study	Chironomids	Füramoos	Mean July air temp.	9.5–14	12–13	12–14	12–16	Unconformity	7–8.5
Ponel (1995)	Beetles	La Grande Pile	MTW	12–25	N/A	11–25	13–26	Not compared	8–12
Behre *et al.* (2005)	Beetles	Oerel	TMAX	9–26	N/A	11–24	N/A		N/A
			TMAXcal	11–19	N/A	16–19	N/A		N/A
Walkling & Coope (1996)	Beetles	Gröbern	TMAXcal	11.5–17	8.5–15	13.5–15	N/A		N/A
Kühl & Litt (2003)	Pollen	La Grande Pile	July temp.	N/A	N/A	15–18	18–19.5		N/A
		Bispingen	July temp.	N/A	N/A	14.5–17.5	16.5–17.5		N/A
		Gröbern	July temp.	N/A	N/A	15	16.5–17		13
Klotz *et al.* (2004)	Pollen	Jammertal	MTW	9.5–20.5	10–18.5	15.5–17.5	15.5–18.5		N/A
		Les Echets	MTW	13.5–20.5	13.5–20.5	14.5–17	16–18.5		N/A
		Füramoos	MTW	11.5–19	11–16	10–17	16–17		N/A
		Samerberg	MTW	10.5–19	11–21.5	10.5–21.5	16–19.5		N/A
Kühl *et al.* (2007)	Pollen	Gröbern	MTW	16.5–17.5	12.5–18	14.5–17.5	17–18		N/A
Müller *et al.* (2003)	Pollen	Jammertal	Summer temp.	11.5–19.5	11.5–21	17–18	18.5		11–13.5
Klotz *et al.* (2003)	Pollen	La Flachère	MTW	8–18	10–22	10–19	16.5–19		N/A
		Lathuile	MTW	12–8	12–18	15–19	14–18.5		16–18.5
		Meikirch II	MTW	N/A	N/A	12–20	15.5–18		11.5–17.5
		Beerenmösli	MTW	12–17	10–18.5	10–18.5	14–18.5		5–17.5
		Jammertal	MTW	11–20	11–17.5	12–17	16–18		13–21.5
		Füramoos	MTW	11–19.5	11.5–15.5	13.5–17	15–19		14–22.5
		Eurach	MTW	N/A	N/A	13.5–18	15–18		10–19
		Samerberg	MTW	11.5–18	11–18.5	15–18.5	14–19		11–16.5
		Zeifen	MTW	N/A	N/A	N/A	15–18		11–20.5
Zagwijn (1996)	Pollen and macrofossils	31 European sites	Summer temp.	N/A	N/A	13.5	17		10

climatic range reconstructions of mean temperature of the warmest month from 11–24 to 16–19 °C from Oerel, northern Germany, for the Late Eemian (Table 1) but regard the calibrated temperatures as being 'rather high'. Nevertheless, many of the estimated summer temperature ranges presented in Table 1 show an overlap with the chironomid-based temperatures, even more so when the error of the chironomid-based temperature reconstruction (±1.3–1.4 °C) is taken into account.

Stadial A. – The chironomid-based July air temperature values for Füramoos during Stadial A (104.5–110 ka) of 12–13 °C are similar to the reconstructed late Eemian temperatures of 12–14 °C. These results are comparable with the beetle-based reconstruction of Walkling & Coope (1996) who indicate a calibrated temperature range of 8.5–15 °C for the Herning stadial (correlated to Stadial A). Overall the summer temperature ranges produced by the pollen-based reconstructions remain rather broad displaying temperatures of 10–21.5 °C, the lower limits of which are in good agreement with the 12–13 °C chironomid-based July air temperature reconstruction while the upper ranges of the pollen-based summer temperature reconstructions are considerably higher than chironomid-based estimates.

Brörup. – The Füramoos chironomid record describes a temperature range of 9.5–14 °C for the Brörup interval; however, the cooling at 799–797 cm is not currently considered representative (Fig. 4) and without those two samples the temperature range is 12–14 °C. Comparisons for the Brörup interstadial should be treated with some caution as the new chironomid record does not cover the entire Brörup interval and neither do all of the pollen-based temperature reconstructions (e.g. Müller *et al.* 2005). However, chironomid-based July air temperature reconstruction ranges produced for our new Füramoos record are within the estimated summer temperature ranges of both the beetle- and pollen-based summer temperature reconstructions (Table 1).

Synoptic temperature and climatic development for the Eemian, Stadial A and Brörup

Our new chironomid-based temperature reconstruction shows long term variations in reconstructed summer

temperatures including the cold temperatures inferred for the late Rissian, relatively high temperatures reconstructed for the mid-Eemian and lower temperatures inferred for the late Eemian and earliest Würmian sections of the record. This agrees with expected temperature changes for these time periods based on other palaeoclimatic evidence (e.g. Ponel 1995; Kühl & Litt 2003; Kühl *et al*. 2007). The most pronounced reconstructed temperature decrease within the Eemian in the chironomid-inferred July air temperature reconstruction, from 16 to 12 °C, is at the transition from the mid- to late Eemian and is associated with decreasing Northern Hemisphere summer insolation (Fig. 6; Berger & Loutre 1991). This suggests that decreasing July temperatures from the mid- to late Eemian may have been a consequence of decreasing summer insolation across this interval. Above we suggest that July air temperature change could have influenced the vegetational transition from the mid- to late Eemian and caused or reinforced the observed shift from a vegetation dominated by *Carpinus* and *Abies* to one dominated by *Pinus* and *Picea*. Bolland *et al*. (2020, 2021) also describe two examples of major chironomid-inferred July air temperature changes within the last glacial interval from Burgäschisee, Swiss plateau (16–14 cal. a BP), and Füramoos (approximately 84–76 ka), that were both associated with changes in Northern Hemisphere July insolation (Berger & Loutre 1991) and pollen evidence of major vegetation change. However, Brewer *et al*. (2008) indicate an increase in seasonality at the mid- to late Eemian transition based on an analysis of 17 European terrestrial pollen records, including the one from Füramoos, and indicate that this increased seasonality was driven by decreases in mean temperature of the coldest month. The transition from *Carpinus* and *Abies* forests to *Pinus* and *Picea* forests at Füramoos could therefore have been influenced by decreasing summer air temperatures, increasing seasonality or both.

Greenland stadial (GS) and interstadial (GI) events are recognized as decadal- to centennial-scale shifts in $\delta^{18}O$ in the Greenland ice-core records covering the Würmian glaciation and the very youngest sections of the Eemian (Rasmussen *et al*. 2014), many of which are observed in speleothem records such as the NALPS record from central Europe (Boch *et al*. 2011; Moseley *et al*. 2020). Several of these stages have been correlated to stadial and interstadial intervals from central European pollen records also (e.g. Müller *et al*. 2003; Fletcher *et al*. 2010). There are possibly three GS stages that could coincide with decreases in chironomid-inferred temperature in the Fu15-2 core, GS 26, 25 and 24 (Fig. 6). GS 26 has a similar age as the transition from the mid- to late Eemian and the largest temperature decrease in the chironomid-inferred July air temperature reconstruction from 16 to 12 °C. Although changes in the NALPS speleothem record are very minor during GS 26, this event may possibly have reinforced the cooling trend during the mid-Eemian recorded at Füramoos. GS 25 is recorded as a short-lived decrease in $\delta^{18}O$ in the NALPS speleothem record and may possibly be associated with a very minor reconstructed temperature decrease at the beginning of Stadial A from 14 to 12.5 °C, although temperatures in Stadial A are almost entirely within the reconstructed error margins of the late Eemian temperature reconstructions. Finally, earlier research has linked GS 24 to the Montaigu event (Woillard 1978; Müller *et al*. 2003), a well-documented stadial interval in central European pollen records within the Brörup interstadial. The decrease observed in the chironomid-based July air temperature reconstruction between 799 and 797 cm could possibly be representative of the Montaigu event. However as discussed, this decrease is considered uncertain and the Brörup section of the core remains temporally poorly constrained.

Conclusions

We present a new chironomid-based July air temperature reconstruction from Füramoos, southern Germany, yielding temperature estimates from the late Rissian, the Eemian interglacial, Stadial A, and the Brörup interstadial. Our chironomid-based reconstructions are augmented by palynological information from the same core. The Rissian part of the examined core is characterized by summer temperatures of 7–9 °C associated with open tundras. Mid-Eemian July air temperatures decrease from 16 to 12 °C at the transition to the Late Eemian, which is reconstructed to have July air temperatures of 12–14 °C. July air temperatures were at 12–13 °C in Stadial A and remained at 12–14 °C in the Brörup interstadial.

In general, the summer temperature decrease associated with the transition from the mid-Eemian to the late Eemian is in agreement with previously available central European temperature reconstructions. However overall pollen-based reconstruction methods tend to infer higher temperatures than observed in the new chironomid record. The most pronounced decrease in July air temperature within the Eemian was associated with decreasing July insolation and the transition from a thermophilic mid-Eemian forest to a coniferous late Eemian forest at Füramoos. The new chironomid-based temperature reconstruction from Füramoos provides valuable corroboration and new quantification of temperature development from the late Rissian as well as the interval from the mid-Eemian to the early Brörup interstadial in the alpine foreland of southern Germany.

Acknowledgements. – We thank all members of the field work team including Tobias Fischer, Ulrich Kotthoff and Bertil Mächtle who helped in retrieving the Fu15-1 and 2 cores from Füramoos and also thank Susanne Liner for technical support. We also thank the two anonymous reviewers and editor whose comments helped improve and

clarify this manuscript. The generosity and support of Franz Fischer (Füramoos) in providing access to the coring site is gratefully acknowledged. This research has been supported by the Swiss National Science Foundation (SNF grant 200021_165494).

Author contributions. – AB: conceptualization, methodology, validation, formal analysis, writing – original draft, project administration, investigation, data curation, visualization, resources, writing – review and editing. OH: conceptualization, methodology, validation, formal analysis, writing – original draft, project administration, supervision, writing – review and editing, funding acquisition, supervision. OK: investigation, resources, writing – review and editing. AK: resources, writing – review and editing, supervision. JP: resources, writing – review and editing, supervision.

Data availability statement. – Chironomid data associated with this study as well as the chironomid-inferred temperature data will be deposited in the Dryad online data repository: https://doi.org/10.5061/dryad.8cz8w9gpt.

References

Andersen, T., Cranston, P. S. & Epler, J. H. 2013: Chironomidae of the Holarctic region: keys and diagnoses: larvae. *Insect Systematics & Evolution, Supplement 66*, 1–571.

de Beaulieu, J. L. & Reille, M. 1984: A long upper Pleistocene pollen record from Les Echets, near Lyon, France. *Boreas 13*, 111–132.

de Beaulieu, J. L. & Reille, M. 1992a: The last climatic cycle at La Grande Pile (Vosges, France France) a new pollen profile. *Quaternary Science Reviews 11*, 431–438.

de Beaulieu, J. L. & Reille, M. 1992b: Long Pleistocene pollen sequences from the Velay Plateau (Massif Central, France). *Vegetation History and Archaeobotany 1*, 233–242.

Beck, P., Caudullo, G., de Rigo, D. & Tinner, W. 2016: Betula pendula, Betula pubescens and other birches in Europe: distribution, habitat, usage and threats. *In* San-Miguel-Ayanz, J., de Rigo, D., Caudullo, G., Houston Durrant, T. & Mauri, A. (eds.): *European Atlas of Forest Tree Species*, 70–73. Publication Office of the European Union, Luxembourg.

Becker, C. 2018: *Vegetations-und Klimaentwicklung in Süddeutschland während des Letzten Interglazial-Komplexes anhand neuer Bohrkerne aus Füramoos (Oberschwaben)*. M.Sc. thesis, Heidelberg University, 68 pp.

Behre, K. E., Hölzer, A. & Lemdahl, G. 2005: Botanical macro-remains and insects from the Eemian and Weichselian site of Oerel (northwest Germany) and their evidence for the history of climate. *Vegetation History and Archaeobotany 14*, 31–53.

Bennett, K. D. 1996: Determination of the number of zones in a biostratigraphical sequence. *New Phytologist 132*, 155–170.

Berger, A. & Loutre, M. F. 1991: Insolation values for the climate of the last 10 million years. *Quaternary Science Reviews 10*, 297–317.

Bińka, K. & Nitychoruk, J. 2001: Late Saalian climate changes in Europe in the light of pollen analysis and the problem of two-step deglaciation at the oxygen isotope stage 6/5e transition. *Boreas 30*, 307–316.

Birks, H. J. B., Braak, C. T., Line, J. M., Juggins, S. & Stevenson, A. C. 1990: Diatoms and pH reconstruction. *Philosophical Transactions of the Royal Society B: Biological Sciences 327*, 263–278.

Birks, H. J. B., Heiri, O., Seppä, H. & Bjune, A. E. 2010: Strengths and weaknesses of quantitative climate reconstructions based on Late–Quaternary Biological Proxies. *The Open Ecology Journal 3*, 68–100.

Boch, R., Cheng, H., Spötl, C., Edwards, R. L., Wang, X. & Häuselmann, P. 2011: NALPS: a precisely dated European climate record 120–60 ka. *Climate of the Past 7*, 1247–1259.

Bolland, A., Kern, O. A., Allstädt, F. J., Peteet, D., Koutsodendris, A., Pross, J. & Heiri, O. 2021: Summer temperatures during the last glaciation (MIS 5c to MIS 3) inferred from a 50,000-year chironomid record from Füramoos, southern Germany. *Quaternary Science Reviews 264*, 107008, https://doi.org/10.1016/j.quascirev.2021.107008.

Bolland, A., Rey, F., Gobet, E., Tinner, W. & Heiri, O. 2020: Summer temperature development 18000–14000 cal. BP recorded by a new chironomid record from Burgäschisee, Swiss Plateau. *Quaternary Science Reviews 243*, 106484, https://doi.org/10.1016/j.quascirev.2020.106484.

ter Braak, C. J. & Juggins, S. 1993: Weighted averaging partial least squares regression (WA-PLS): an improved method for reconstructing environmental variables from species assemblages. *Hydrobiologia 269*, 485–502.

ter Braak, J. F. & Smilauer, P. 2018: *Canoco Reference Manual and User's Guide: Software for Ordination (version 5.10)*. 376 pp. Microcomputer Power, Ithaca.

ter Braak, C. J. F., Juggins, S., Birks, H. J. B. & Van der Voet, H. 1993: Weighted averaging partial least squares regression (WA-PLS): definition and comparison with other methods for species-environment calibration. *In* Patil, G. P. & Rao, C. R. (eds.): *Multivariate Environmental Statistics*, 525–560. Elsevier Science Publishers, Amsterdam.

Brewer, S., Guiot, J., Sánchez-Goñi, M. F. & Klotz, S. 2008: The climate in Europe during the Eemian: a multi-method approach using pollen data. *Quaternary Science Reviews 27*, 2303–2315.

Brodersen, K. P. & Anderson, N. J. 2002: Distribution of chironomids (Diptera) in low arctic West Greenland lakes: trophic conditions, temperature and environmental reconstruction. *Freshwater Biology 47*, 1137–1157.

Brodersen, K. P. & Lindegaard, C. 1999: Mass occurance [sic] and sporadic distribution of Corynocera ambigua Zetterstedt (Diptera, Chironomidae) in Danish lakes. Neo-and palaeolimnological records. *Journal of Paleolimnology 22*, 41–52.

Brodersen, K. P., Pedersen, O., Lindegaard, C. & Hamburger, K. 2004: Chironomids (Diptera) and oxy-regulatory capacity: an experimental approach to paleolimnological interpretation. *Limnology and Oceanography 49*, 1549–1559.

Brodin, Y. W. 1986: The postglacial history of Lake Flarken, southern Sweden, interpreted from subfossil insect remains. *Internationale Revue der gesamten Hydrobiologie und Hydrographie 71*, 371–432.

Brooks, S. J. 2006: Fossil midges (Diptera: Chironomidae) as palaeoclimatic indicators for the Eurasian region. *Quaternary Science Reviews 25*, 1894–1910.

Brooks, S. J. & Birks, H. J. B. 2000: Chironomid-inferred late-glacial and early-Holocene mean July air temperatures for Kråkenes Lake, northwestern Norway. *Journal of Paleolimnology 23*, 77–89.

Brooks, S. J., Langdon, P. G. & Heiri, O. 2007: The identification and use of Palaearctic Chironomidae larvae in palaeoecology. *Quaternary Research Association, Technical Guide Number 10*, 276 pp.

Brundin, L. 1949: Chironomiden und andere Bodentiere der südschwedischen Urgebirgseen. Ein Beitrag zur Kenntnis der bodenfaunistischen Charakterzüge schwedischer oligotropher Seen. *Report of the Institute of Freshwater Research, Drottningholm 30*, 1–914.

Busschers, F. S., Van Balen, R. T., Cohen, K. M., Kasse, C., Weerts, H. J., Wallinga, J. & Bunnik, F. P. 2008: Response of the Rhine-Meuse fluvial system to Saalian ice-sheet dynamics. *Boreas 37*, 377–398.

Caudullo, G., Tinner, W. & de Rigo, D. 2016: Picea abies in Europe: distribution, habitat, usage and threats. *In* San-Miguel-Ayanz, J., de Rigo, D., Caudullo, G., Houston Durrant, T. & Mauri, A. (eds.): *European Atlas of Forest Tree Species*, 114–116. Publications Office of the European Union, Luxembourg.

Cheddadi, R., Mamakowa, K., Guiot, J., De Beaulieu, J. L., Reille, M., Andrieu, V., Granoszewski, W. & Peyron, O. 1998: Was the climate of the Eemian stable? A quantitative climate reconstruction from seven European pollen records. *Palaeogeography, Palaeoclimatology, Palaeoecology 143*, 73–85.

Dansgaard, W., Johnsen, S. J., Clausen, H. B., Dahl-Jensen, D., Gundestrup, N. S., Hammer, C. U., Hvidberg, C. S., Steffensen, J. P., Sveinbjörnsdottir, A. E., Jouzel, J. & Bond, G. 1993: Evidence for general instability of past climate from a 250-kyr ice-core record. *Nature 364*, 218–220.

Durrant, T. H., de Rigo, D. & Caudullo, G. 2016: *Pinus sylvestris* in Europe: distribution, habitat, usage and threats. *In* San Miguel Ayanz, J., de Rigo, D., Caudullo, G., Houston Durrant, T. & Mauri,

A. (eds.): *European Atlas of Forest Tree Species*, 132–133. Publication Office of the European Union, Luxembourg.

Dutton, A., Carlson, A. E., Long, A., Milne, G. A., Clark, P. U., DeConto, R., Horton, B. P., Rahmstorf, S. & Raymo, M. E. 2015: Sea-level rise due to polar ice-sheet mass loss during past warm periods. *Science 349*, 6244, https://doi.org/10.1126/science.aaa4019.

DWD Climate Data Center (CDC). 2021: Historische monatliche Stationsbeobachtungen (Temperatur, Druck, Niederschlag, Sonnenscheindauer, etc.) für Deutschland, Version v21.3. https://cdc.dwd.de/portal/.

Eggermont, H. & Heiri, O. 2012: The chironomid-temperature relationship: expression in nature and palaeoenvironmental implications. *Biological Reviews 87*, 430–456.

Eisele, G., Haas, K. & Liner, S. 1994: Methode zur Aufbereitung fossilen Pollens aus minerogenen Sedimenten. *In* Frenzel, B. (ed.): *Über Probleme der holozänen vegetationsgeschichte Osttibets 95*, 165–166. Göttinger Geographische Abhandlungen, Göttingen.

Engels, S. & Cwynar, L. C. 2011: Changes in fossil chironomid remains along a depth gradient: evidence for common faunal thresholds within lakes. *Hydrobiologia 665*, 15–38.

Engels, S., Bohncke, S. J. P., Bos, J. A. A., Brooks, S. J., Heiri, O. & Helmens, K. F. 2008: Chironomid-based palaeotemperature estimates for northeast Finland during Oxygen Isotope Stage 3. *Journal of Paleolimnology 40*, 49–61.

Engels, S., Helmens, K. F., Väliranta, M., Brooks, S. J. & Birks, H. J. B. 2010: Early Weichselian (MIS 5d and 5c) temperatures and environmental changes in northern Fennoscandia as recorded by chironomids and macroremains at Sokli, northeast Finland. *Boreas 39*, 689–704.

Engels, S., Self, A. E., Luoto, T. P., Brooks, S. J. & Helmens, K. F. 2014: A comparison of three Eurasian chironomid–climate calibration datasets on a W-E continentality gradient and the implications for quantitative temperature reconstructions. *Journal of Paleolimnology 51*, 529–547.

Field, M. H., Huntley, B. & Müller, H. 1994: Eemian climate fluctuations observed in a European pollen record. *Nature 371*, 779–783.

Fletcher, W. J., Sanchez Goñi, M. F., Peyron, O. & Dormoy, I. 2010: Abrupt climate changes of the last deglaciation detected in a Western Mediterranean forest record. *Climate of the Past 6*, 245–264.

Francis, D. R. 2001: Bryozoan statoblasts. *In* Smol, J. P., Birks, H. J. B. & Last, W. M. (eds.): *Tracking Environmental Change Using Lake Sediments. Volume 4: Zoological Indicators*, 105–123. Kluwer Academic Publishers, Dordrecht.

Frey, D. G. 1988: Littoral and offshore communities of diatoms, cladocerans and dipterous larvae, and their interpretation in paleolimnology. *Journal of Paleolimnology 1*, 179–191.

Grimm, E. C. 1987: CONISS: A Fortran 77 program for stratigraphically constrained cluster analysis by the method of incremental sum of squares. *Computers & Geosciences 13*, 13–35.

Grüger, E. 1979: Spätriss, Riss/Würm und Frühwürm am Samerberg in Oberbayern — ein vegetationsgeschichtlicher Beitrag zur Gliederung des Jungpleistozäns. *Geologica Bavarica 80*, 5–64.

Guiot, J., Pons, A., de Beaulieu, J. L. & Reille, M. 1989: A 140,000-year continental climate reconstruction from two European pollen records. *Nature 338*, 309–313.

Haas, J. N. 1994: First identification key for charophyte oospores from central Europe. *European Journal of Phycology 29*, 227–235.

Heggen, M. P., Birks, H. H., Heiri, O., Grytnes, J. A. & Birks, H. J. B. 2012: Are fossil assemblages in a single sediment core from a small lake representative of total deposition of mite, chironomid, and plant macrofossil remains? *Journal of Paleolimnology 48*, 669–691.

Heiri, O. & Lotter, A. F. 2001: Effect of low count sums on quantitative environmental reconstructions: an example using subfossil chironomids. *Journal of Paleolimnology 26*, 343–350.

Heiri, O. & Lotter, A. F. 2010: How does taxonomic resolution affect chironomid-based temperature reconstruction? *Journal of Paleolimnology 44*, 589–601.

Heiri, O., Birks, H. J. B., Brooks, S. J., Velle, G. & Willassen, E. 2003: Effects of within-lake variability of fossil assemblages on quantitative chironomid-inferred temperature reconstruction. *Palaeogeography, Palaeoclimatology, Palaeoecology 199*, 95–106.

Heiri, O., Brooks, S. J., Birks, H. J. B. & Lotter, A. F. 2011: A 274-lake calibration data-set and inference model for chironomid-based summer air temperature reconstruction in Europe. *Quaternary Science Reviews 30*, 3445–3456.

Heiri, O., Lotter, A. F. & Lemcke, G. 2001: Loss on ignition as a method for estimating organic and carbonate content in sediments: reproducibility and comparability of results. *Journal of Paleolimnology 25*, 101–110.

Hofmann, W. 2001: Late-Glacial/Holocene succession of the chironomid and cladoceran fauna of the Soppensee (Central Switzerland). *Journal of Paleolimnology 25*, 411–420.

Ilyashuk, E. A., Ilyashuk, B. P., Heiri, O. & Spötl, C. 2020: Summer temperatures and lake development during the MIS 5a interstadial: new data from the Unterangerberg palaeolake in the Eastern Alps, Austria. *Palaeogeography, Palaeoclimatology, Palaeoecology 560*, 110020, https://doi.org/10.1016/j.palaeo.2020.110020.

Johnsen, S. J., Clausen, H. B., Dansgaard, W., Gundestrup, N. S., Hammer, C. U., Andersen, U., Andersen, K. K., Hvidberg, C. S., Dahl-Jensen, D., Steffensen, J. P. & Shoji, H. 1997: The $\delta^{18}O$ record along the Greenland Ice Core Project deep ice core and the problem of possible Eemian climatic instability. *Journal of Geophysical Research: Oceans 102*, 26397–26410.

Juggins, S. 2007: *C2: Software for Ecological and Palaeoecological Data Analysis and Visualisation (User Guide Version 1.5)*. 73 pp. Newcastle University, Newcastle upon Tyne.

Juggins, S. 2017: *Rioja: Analysis of Quaternary Science Data, R package version (0.9-21)*. http://cran.r-project.org/package=rioja.

Kern, O. A., Koutsodendris, A., Mächtle, B., Christanis, K., Schukraft, G., Scholz, C., Kotthoff, U. & Pross, J. 2019: XRF core scanning yields reliable semiquantitative data on the elemental composition of highly organic-rich sediments: evidence from the Füramoos peat bog (Southern Germany). *Science of the Total Environment 697*, 134110, https://doi.org/10.1016/j.scitotenv.2019.134110.

Klotz, S., Guiot, J. & Mosbrugger, V. 2003: Continental European Eemian and early Würmian climate evolution: comparing signals using different quantitative reconstruction approaches based on pollen. *Global and Planetary Change 36*, 277–294.

Klotz, S., Müller, U., Mosbrugger, V., de Beaulieu, J. L. & Reille, M. 2004: Eemian to early Würmian climate dynamics: history and pattern of changes in Central Europe. *Palaeogeography, Palaeoclimatology, Palaeoecology 211*, 107–126.

Kühl, N. & Litt, T. 2003: Quantitative time series reconstruction of Eemian temperature at three European sites using pollen data. *Vegetation History and Archaeobotany 12*, 205–214.

Kühl, N., Litt, T., Schölzel, C. & Hense, A. 2007: Eemian and Early Weichselian temperature and precipitation variability in northern Germany. *Quaternary Science Reviews 26*, 3311–3317.

Landolt, E. 2003: *Unsere Alpenflora*. 353 pp. Gustav Fischer, Stuttgart.

Lemdahl, G. 2000: Lateglacial and Early Holocene insect assemblages from sites at different altitudes in the Swiss Alps – implications on climate and environment. *Palaeogeography, Palaeoclimatology, Palaeoecology 159*, 293–312.

Litt, T. 1994: Paläoökologie, Paläobotanik und Stratigraphie des Jungquartärs im nordmitteleuropäischen Tiefland. *Dissertationes Botanicae 227*, 185 pp.

Lotter, A. F., Heiri, O., Brooks, S., van Leeuwen, J. F., Eicher, U. & Ammann, B. 2012: Rapid summer temperature changes during Termination 1a: high-resolution multi-proxy climate reconstructions from Gerzensee (Switzerland). *Quaternary Science Reviews 36*, 103–113.

Lotter, A. F., Walker, I. R., Brooks, S. J. & Hofmann, W. 1999: An intercontinental comparison of chironomid palaeotemperature inference models: Europe vs North America. *Quaternary Science Reviews 18*, 717–735.

Luoto, T. P. 2009: Subfossil Chironomidae (Insecta: Diptera) along a latitudinal gradient in Finland: development of a new temperature inference model. *Journal of Quaternary Science 24*, 150–158.

Luoto, T. P., Kotrys, B. & Płóciennik, M. 2019: East European chironomid-based calibration model for past summer temperature reconstructions. *Climate Research 77*, 63–76.

Lüthi, D., Le Floch, M., Bereiter, B., Blunier, T., Barnola, J. M., Siegenthaler, U., Raynaud, D., Jouzel, J., Fischer, H., Kawamura, K. & Stocker, T. F. 2008: High-resolution carbon dioxide concentration record 650,000–800,000 years before present. *Nature 453*, 379–382.

Masson-Delmotte, V., Schulz, M., Abe-Ouchi, A., Beer, J., Ganopolski, A., González Rouco, J. F., Jansen, E., Lambeck, K., Luterbacher, J., Naish, T., Osborn, T., Otto-Bliesner, B., Quinn, T., Ramesh, R., Rojas, M., Shao, X. & Timmermann, A. 2013: Information from paleoclimate archives. *In* Stocker, T. F., Qin, D., Plattner, G. K., Tignor, M., Allen, S. K., Boschung, J., Nauels, A., Xia, Y., Bex, V. & Midgley, P. M. (eds.): *Climate Change 2013: The Physical Science Basis*. 383–465. Cambridge University Press, Cambridge.

McGarrigle, M. L. 1980: The distribution of chironomid communities and controlling sediment parameters in L. Derravaragh, Ireland. *In* Murray, D. A. (ed.): *Chironomidae: Ecology, Systematics, Cytology, and Physiology*, 275–282. Pergamon Press, Oxford.

Millet, L., Vannière, B., Verneaux, V., Magny, M., Disnar, J. R., Laggoun-Défarge, F., Walter-Simonnet, A. V., Bossuet, G., Ortu, E. & de Beaulieu, J. L. 2007: Response of littoral chironomid communities and organic matter to late glacial lake—level, vegetation and climate changes at Lago dell'Accesa (Tuscany, Italy). *Journal of Paleolimnology 38*, 525–539.

Moseley, G. E., Spötl, C., Brandstätter, S., Erhardt, T., Luetscher, M. & Edwards, R. L. 2020: NALPS19: sub-orbital-scale climate variability recorded in northern Alpine speleothems during the last glacial period. *Climate of the Past 16*, 29–50.

Müller, U. C. 2000: A Late-Pleistocene pollen sequence from the Jammertal, south-western Germany with particular reference to location and altitude as factors determining Eemian forest composition. *Vegetation History and Archaeobotany 9*, 125–131.

Müller, U. C., Klotz, S., Geyh, M. A., Pross, J. & Bond, G. C. 2005: Cyclic climate fluctuations during the last interglacial in central Europe. *Geology 33*, 449–452.

Müller, U. C., Pross, J. & Bibus, E. 2003: Vegetation response to rapid climate change in Central Europe during the past 140,000 yr based on evidence from the Füramoos pollen record. *Quaternary Research 59*, 235–245.

Nazarova, L., Bleibtreu, A., Hoff, U., Dirksen, V. & Diekmann, B. 2017: Changes in temperature and water depth of a small mountain lake during the past 3000 years in Central Kamchatka reflected by a chironomid record. *Quaternary International 447*, 46–58.

Nazarova, L., Self, A. E., Brooks, S. J., van Hardenbroek, M., Herzschuh, U. & Diekmann, B. 2015: Northern Russian chironomid-based modern summer temperature data set and inference models. *Global and Planetary Change 134*, 10–25.

Otto-Bliesner, B. L., Rosenbloom, N., Stone, E. J., McKay, N. P., Lunt, D. J., Brady, E. C. & Overpeck, J. T. 2013: How warm was the last interglacial? New model–data comparisons. *Philosophical Transactions of the Royal Society A: Mathematical, Physical and Engineering Sciences 371*, 20130097, https://doi.org/10.1098/rsta.2013.0097.

Plikk, A., Engels, S., Luoto, T. P., Nazarova, L., Salonen, J. S. & Helmens, K. F. 2019: Chironomid-based temperature reconstruction for the Eemian Interglacial (MIS 5e) at Sokli, northeast Finland. *Journal of Paleolimnology 61*, 355–371.

Ponel, P. 1995: Rissian, Eemian and Würmian Coleoptera assemblages from La Grande Pile (Vosges, France). *Palaeogeography, Palaeoclimatology, Palaeoecology 114*, 1–41.

R Studio Team 2015: *RStudio: Integrated Development for R*. RStudio, Inc., Boston, MA, http://www.rstudio.com/.

Rasmussen, S. O., Bigler, M., Blockley, S. P., Blunier, T., Buchardt, S. L., Clausen, H. B., Cvijanovic, I., Dahl-Jensen, D., Johnsen, S. J., Fischer, H., Gkinis, V., Guillevic, M., Hoek, W. Z., Lowe, J. J., Pedro, J. B., Popp, T., Seierstad, I. K., Steffensen, J. P., Svensson, A. M., Vallelonga, P., Vinther, B. M., Walker, M. J. C., Wheatley, J. J. & Winstrup, M. 2014: A stratigraphic framework for abrupt climatic changes during the Last Glacial period based on three synchronized Greenland ice-core records: refining and extending the INTIMATE event stratigraphy. *Quaternary Science Reviews 106*, 14–28.

Reille, M. & De Beaulieu, J. L. 1990: Pollen analysis of a long upper Pleistocene continental sequence in a Velay maar (Massif Central, France). *Palaeogeography, Palaeoclimatology, Palaeoecology 80*, 35–48.

de la Riva-Caballero, A., Birks, H. J. B., Bjune, A. E., Birks, H. H. & Solhøy, T. 2010: Oribatid mite assemblages across the tree-line in western Norway and their representation in lake sediments. *Journal of Paleolimnology 44*, 361–374.

Saether, O. A. 1979: Chironomid communities as water quality indicators. *Ecography 2*, 65–74.

Samartin, S., Heiri, O., Joos, F., Renssen, H., Franke, J., Brönnimann, S. & Tinner, W. 2017: Warm Mediterranean mid-Holocene summers inferred from fossil midge assemblages. *Nature Geoscience 10*, 207–212.

Schilt, A., Baumgartner, M., Schwander, J., Buiron, D., Capron, E., Chappellaz, J., Loulergue, L., Schüpbach, S., Spahni, R., Fischer, H. & Stocker, T. F. 2010: Atmospheric nitrous oxide during the last 140,000 years. *Earth and Planetary Science Letters 300*, 33–43.

Schmid, P. E. 1993: *A key to the larval Chironomidae and their instars from Austrian Danube region streams and rivers: with particular reference to a numerical taxonomic approach. 1. Diamesinae, Prodiamesinae and Orthocladiinae*. 514 pp. Federal Institute for Water Quality, Wasser und Abwasser, Supplement 3, Vienna.

Schreiner, A. 1982: Quartärgeologische Untersuchungen in der Umgebung von Interglazialvorkommen im östlichen Rheingletschergebiet (Baden-Württemberg). *Geologisches Jahrbuch A 59*, 64 pp.

Schreiner, A. 1996: *Erläuterungen zu 8025 Bad Wurzach: Geologische Karte von Baden-Württemberg 1:25 000*. 1st ed. Landesvermessungsamt Baden-Württemberg, Freiburg.

Shackleton, N. J., Sánchez-Goñi, M. F., Pailler, D. & Lancelot, Y. 2003: Marine isotope substage 5e and the Eemian interglacial. *Global and Planetary Change 36*, 151–155.

Šmilauer, P. & Lepš, J. 2014: *Multivariate Analysis of Ecological Data Using CANOCO 5*. 376 pp. Cambridge University Press, Cambridge.

Solhøy, T. 2001: Oribatid mites. *In* Smol, J. P., Birks, H. J. B. & Last, W. M. (eds.): *Tracking Environmental Change Using Lake Sediments. Volume 4: Zoological Indicators*, 81–104. Kluwer Academic Publishers, Dordrecht.

Stockmarr, J. A. 1971: Tablets with spores used in absolute pollen analysis. *Pollen et Spores 13*, 615–621.

Tóth, M., Magyari, E. K., Buczkó, K., Braun, M., Panagiotopoulos, K. & Heiri, O. 2015: Chironomid-inferred Holocene temperature changes in the South Carpathians (Romania). *Holocene 25*, 569–582.

Turner, C. & West, R. G. 1968: The subdivision and zonation of interglacial periods. *Eiszeitalter und Gegenwart 19*, 93–101.

Turney, C. S. & Jones, R. T. 2010: Does the Agulhas Current amplify global temperatures during super-interglacials? *Journal of Quaternary Science 25*, 839–843.

Vandekerkhove, J., Declerck, S., Vanhove, M., Brendonck, L., Jeppesen, E., Conde Porcuna, J. M. & De Meester, L. 2004: Use of ephippial morphology to assess richness of anomopods: potentials and pitfalls. *Journal of Limnology 63*, 75–84.

Walker, I. R., Smol, J. P., Engstrom, D. R. & Birks, H. J. B. 1991: An assessment of Chironomidae as quantitative indicators of past climatic change. *Canadian Journal of Fisheries and Aquatic Sciences 48*, 975–987.

Walkling, A. P. & Coope, G. R. 1996: Climatic reconstructions from the Eemian/Early Weichselian transition in Central Europe based on the coleopteran record from Gröbern, Germany. *Boreas 25*, 145–159.

Wiederholm, T. 1983: Chironomidae of the Holarctic region: keys and diagnoses: part 1. Larvae. *Entomologica Scandinavica, Supplement 19*, 456 pp.

Winterholler, K. 2004: Zur jungpleistozänen Landschaftsentwicklung am Füramooser Ried (Oberschwaben). *Beiträge zur Geomorphologie, Bodengeographie und Quartärforschung des Geographischen Institut der Universität Tübingen*, 155–180.

Woillard, G. M. 1978: Grande Pile peat bog: a continuous pollen record for the last 140,000 years. *Quaternary Research 9*, 1–21.

Zagwijn, W. H. 1996: An analysis of Eemian climate in western and central Europe. *Quaternary Science Reviews 15*, 451–469.

Supporting Information

Additional Supporting Information may be found in the online version of this article at http://www.boreas.dk.

Fig. S1. Testing sensitivity of the reconstruction in relation to number of chironomid head counts using minimum head count criteria of >30, >40 and >45 head capsules per sample. SA = Stadial A; BR = Brörup.

Data S1. Comparison of reconstructed mean July air temperature values from the FU15 chironomid record at different temporal resolutions.